

Biomicroite, Marlstone, and Shale Properties: Exploration of Nonconventional Hydrocarbons in the Cretaceous Colombian Back-Arc Basin

<https://doi.org/10.32685/pub.esp.36.2019.09>
Published online 25 November 2020

Javier GUERRERO^{1*} , Alejandra MEJÍA-MOLINA² , and José OSORNO³ 

Abstract The nonconventional hydrocarbon potential of the Cretaceous Colombian back-arc basin is explored taking into consideration the properties of fine-grained units, including biomicroite, marlstone, and shale, in terms of total organic carbon content, gas content, vitrinite reflectance, porosity, permeability, pyrolysis, and organic geochemistry of samples collected from outcrop sections and wells in several localities in the core of the Eastern Cordillera, Middle Magdalena Valley, and Catatumbo. The best properties are from the Turonian to Santonian limestones of La Luna Formation and time-equivalent units, but other limestones of Albian and Campanian ages, including the Hilo Formation and the Oliní Group, have potential. La Luna Formation was deposited during a transgressive and relatively high sea level interval; it is composed of biomicroites of planktonic foraminifera, with minor interbedding of marlstones. Diagenetic cherts resulting from replacement of calcite by quartz are also present. The average total organic carbon values of the formation are excellent, between 4.9 and 11.6% for sections in the area of Aguachica, 5.4 to 8.6% in the area of Barichara, and 6.1 to 7.2% in the area of Cúcuta. These high values of total organic carbon are systematically associated with moderate values of thermal maturity, between 0.8 and 1.3% Ro; the interval contains mainly type II kerogen, with minor mixtures of types II–III.

Keywords: Cretaceous, back-arc, nonconventional hydrocarbons, limestones.

Resumen El potencial de hidrocarburos no convencionales de la Cuenca Cretácica Colombiana de back-arc se explora teniendo en cuenta las propiedades de unidades de grano fino, incluyendo biomicroita, marga y lodolita, en términos de contenido de carbono orgánico total, contenido de gas, reflectancia de vitrinita, porosidad, permeabilidad, pirólisis y geoquímica orgánica de muestras recolectadas de secciones de afloramiento y pozos en varias localidades del núcleo de la cordillera Oriental, Valle Medio del Magdalena y Catatumbo. Las mejores propiedades provienen de las calizas del Turoniano al Santoniano de la Formación La Luna y unidades equivalentes en tiempo, pero otras calizas de edades albianas y campanianas, incluyendo la Formación Hilo y el Grupo Oliní, tienen potencial. La Formación La Luna se depositó durante un intervalo transgresivo y relativamente alto del nivel del mar; está compuesta por biomicroitas de foraminíferos planctónicos, con intercalaciones menores de margas. Cherts diagenéticos resultantes del reemplazo de calcita por cuarzo también están presentes. Los valores promedio de carbono orgánico total de la formación son excelentes, entre 4,9 y 11,6 % para seccio-

- 1 jguerrero@unal.edu.co
Universidad Nacional de Colombia
Sede Bogotá
Departamento de Geociencias
Carrera 30 n.º 45-03
Bogotá, Colombia
 - 2 amejia@yachaytech.edu.ec
Universidad Yachay Tech
Hacienda Urcuquí s/n y Proyecto Yachay
Urcuquí, Ecuador
 - 3 jose.osorno@anh.gov.co
Agencia Nacional de Hidrocarburos
Calle 26 n.º 59-65, segundo piso
Bogotá, Colombia
- * Corresponding author

Citation: Guerrero, J., Mejía-Molina, A. & Osorno, J. 2020. Biomicroite, marlstone, and shale properties: Exploration of nonconventional hydrocarbons in the Cretaceous Colombian back-arc basin. In: Gómez, J. & Pinilla-Pachon, A.O. (editors), *The Geology of Colombia, Volume 2 Mesozoic. Servicio Geológico Colombiano, Publicaciones Geológicas Especiales 36*, p. 299–333. Bogotá. <https://doi.org/10.32685/pub.esp.36.2019.09>

nes en el área de Aguachica, 5,4 a 8,6 % en el área de Barichara y 6,1 a 7,2 % en el área de Cúcuta. Estos altos valores de carbono orgánico total se asocian sistemáticamente con valores moderados de madurez térmica, entre 0,8 y 1,3 % Ro; el intervalo contiene principalmente kerógeno tipo II, con mezclas menores de los tipos II–III.

Palabras clave: Cretácico, back-arc, hidrocarburos no convencionales, calizas.

1. Introduction

The distribution of calcareous and terrigenous units, source areas, geochemistry, U–Pb ages, and mineralogy of the Cretaceous Colombian back-arc basin were reported in previous studies (Guerrero 2002a, 2002b; Guerrero *et al.*, 2000, 2020), indicating that the main depositional axis was located in the present day Eastern Cordillera. Limestones are common on the western and northern sides of the basin; in contrast, terrigenous strata predominate on the eastern and southern sides of the basin. Berriasian and Valanginian strata from the lower part of the succession in the main rift were buried at depths of approximately 8 to 9 km and are overmature for oil and gas. Cretaceous strata of younger ages, deposited outside the main rift, in the modern E and W foothills of the Eastern Cordillera, Llanos, and Magdalena Valley, were buried to lower depths and contain most of the hydrocarbons of the basin.

Sandstones and sandy biosparites of the western border are metamorphic and volcanic lithic arenites sourced from the Central Cordillera; sandstones from the eastern side of the basin are quartz arenites sourced mostly from recycled Paleozoic and older strata from the Guiana Shield. In fact, most of the Cretaceous sections rest with angular unconformity on Paleozoic strata on the eastern border of the basin, while they rest with angular unconformity on igneous and volcanoclastic rocks of Jurassic age on the western border of the basin. The Cretaceous strata present today in the Eastern Cordillera of the Colombian Andes were deposited in a back-arc basin (Figure 1) related to subduction perpendicular to the western border of the continent. The remains of the Cretaceous fore-arc basin include strata that overlie accreted oceanic basalts of MORB affinity, present in the Western Cordillera and western side of the Central Cordillera.

The limestones, diagenetic cherts, and marlstones present on the W and N sides of the basin are of major interest because they include important source rocks and constitute nonconventional reservoirs of hydrocarbons. They have a much better quality of marine organic matter than the shales from the S and E sides of the basin. The type and quality of organic matter was controlled by the offshore sedimentary environments (including mud and silt sedimentation under fair weather climate and sporadic storms) and by the availability of terrigenous particles, including clay minerals and silt-sized quartz particles. The terms gas-shale and oil-shale have been imprecisely applied to fine-grained rocks in the range of silt- and clay-sized particles, which could have either biogenic or terrigenous origin. Howev-

er, many of those fine-grained rocks include important carbonate contents and are limestones (mainly biomicrites) instead of shales, so it is a better strategy to explore biomicrites instead of shales and to recognize the major differences between those types of rocks. One very important difference is that the biomicrites are more brittle (and respond better to fracking) than the plastic shales, which contain large amounts of clay minerals; the other difference is that organic matter particles of terrestrial origin, including plant debris, are more common in the shales than in the biomicrites, so that they are more prone to produce gas than the biomicrites that generate mainly oil hydrocarbons. In fact, the presence of centimeter-scale regressive marlstone beds within the dominantly transgressive and high-stand biomicrite parasequences is very important because it introduces large amounts of organic matter of terrestrial origin, producing mixtures of type II and type III organic matter.

The geographic location and stratigraphic position of the studied sections are presented in Figures 1–3 and Tables 1 and 2.

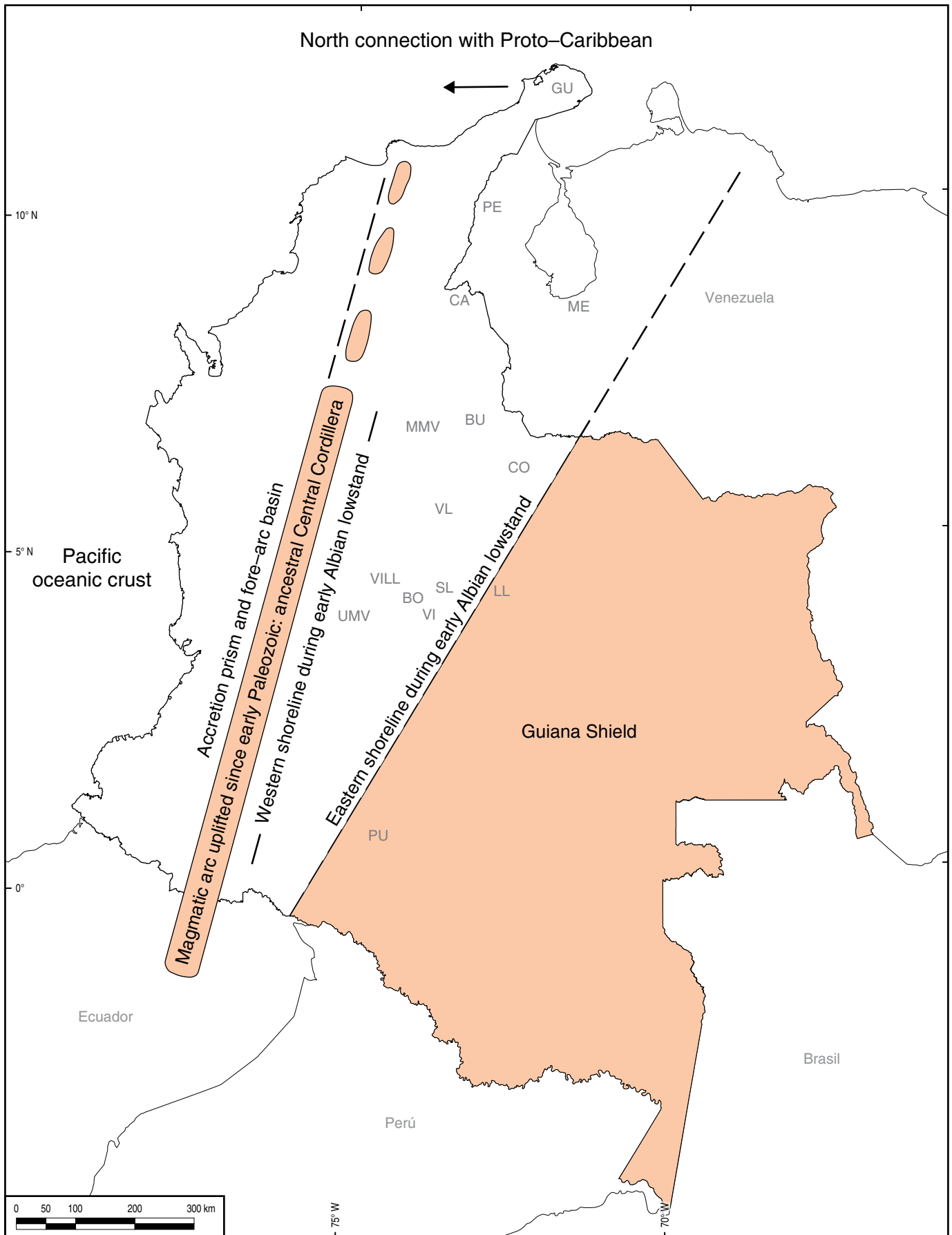
2. Materials and Methods

Fine-grained strata, including biomicrites, marlstones, and shales, were collected from 9 wells and 35 field sections at key localities in the basin. Best exposures with published stratigraphy were picked to minimize stratigraphic mistakes. Pyrolysis, total organic carbon (TOC), porosity, permeability, and organic geochemistry analyses were performed at the Antek S.A. laboratories. A total of 1500 samples were processed for TOC, 1500 for vitrinite reflectance, 500 for pyrolysis, 500 for petrophysics, 500 for biomarkers, and 200 for gas content and chromatography.

3. Results

The total organic carbon (TOC) and thermal maturity (Ro) results of 3000 samples are presented as averages per stratigraphic section, displayed in Table 3. The highest average content (11.6% TOC) in the upper part of the table corre-

Figure 1. Paleogeography of the Cretaceous Colombian back-arc basin during the early Albian. La Guajira was aligned with Santa Marta and the Central Cordillera. Sections are: (PU) Putumayo; (UMV) Upper Magdalena Valley; (LL) Llanos; (VI) Villavicencio; (SL) San Luis; (BO) Bogotá; (VILL) Villeta; (VL) Villa de Leyva; (CO) Cocuy; (BU) Bucaramanga; (MMV) Middle Magdalena Valley; (CA) Catatumbo; (ME) Mérida; (PE) Perijá; (GU) Guajira. Modified from Guerrero (2002a).



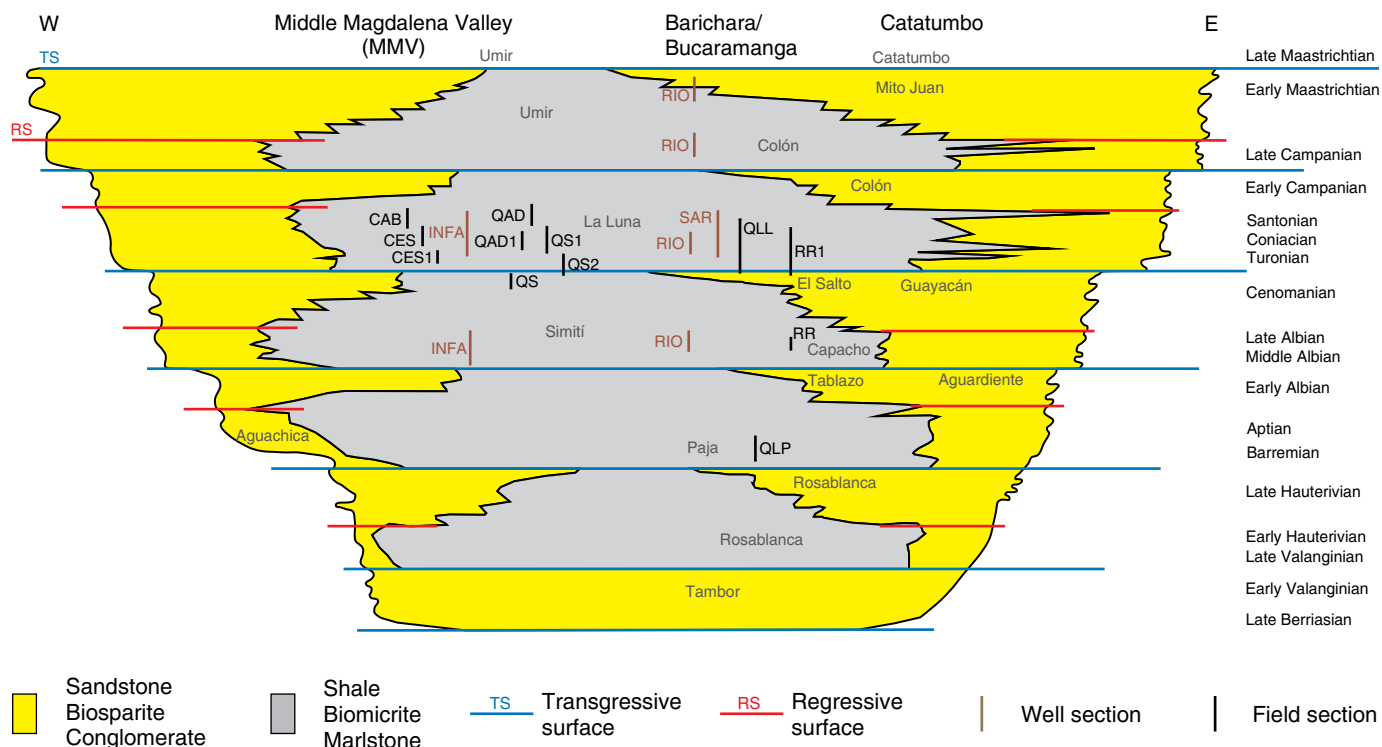


Figure 2. Sections studied in the N sector of the basin, including the Middle Magdalena Valley, Barichara/Bucaramanga, and Catatumbo areas. Modified from Guerrero (2002a).

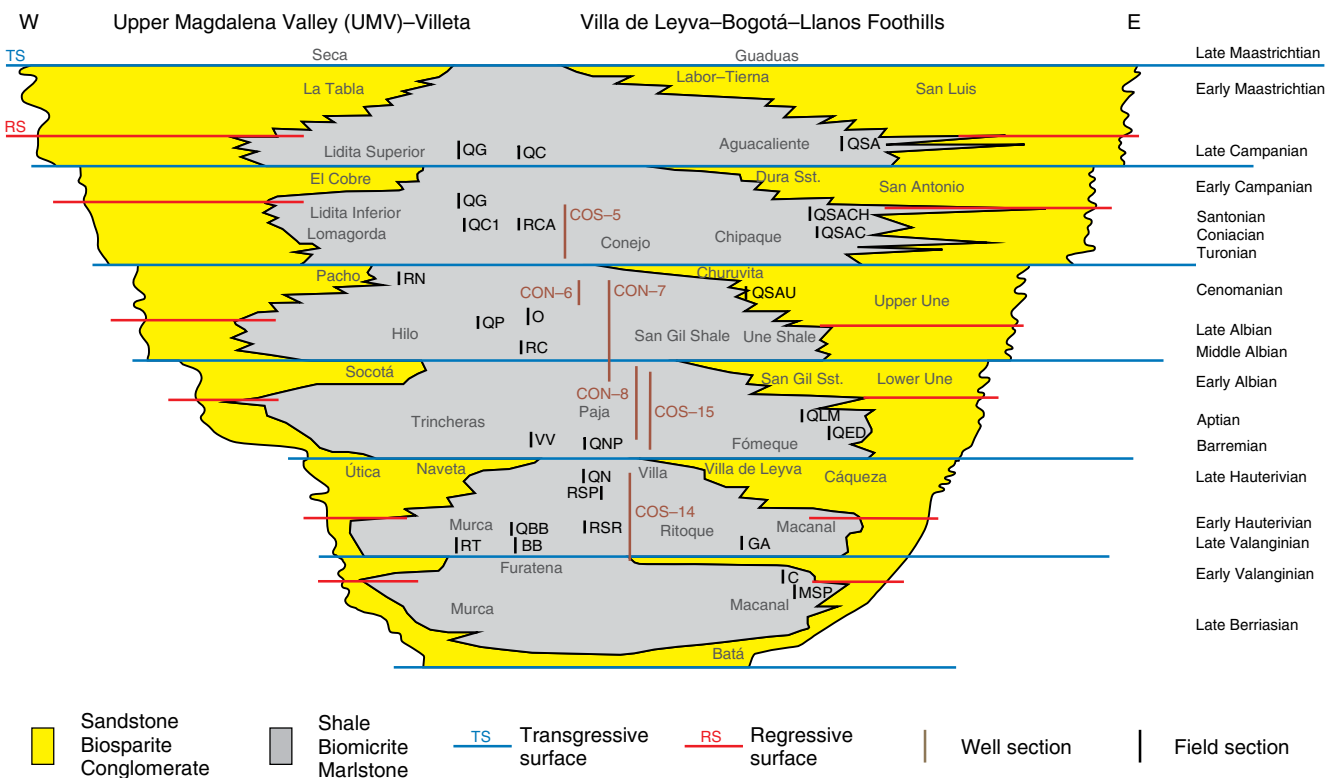


Figure 3. Sections studied in the S sector of the basin, including the Eastern and Western Emerald belts and the Villeta, Villa de Leyva, and Bogotá areas. Modified from Guerrero (2002a).

Table 1. Location of field sections.

Sample	Section	Area	Formation	Age	Latitude N	Longitude W
BB-00	Buriburi	CEOC	Furatena (Lower)	Berriasian – early Hauterivian	5° 40' 28.931"	74° 03' 54.439"
BB-10	Buriburi	CEOC	Furatena (Lower)	Berriasian – early Hauterivian	5° 40' 27.833"	74° 03' 53.743"
C-00	Cachipay	CEOR	Macanal	Berriasian – early Hauterivian	4° 52' 24.791"	73° 14' 18.525"
C-48	Cachipay	CEOR	Macanal	Berriasian – early Hauterivian	4° 52' 23.458"	73° 14' 16.868"
CAB-00	Agua Blanca Creek	Aguachica	La Luna (Upper)	Coniacian to Santonian	8° 13' 28.226"	73° 32' 07.428"
CAB-128	Agua Blanca Creek	Aguachica	La Luna (Upper)	Coniacian to Santonian	8° 13' 25.764"	73° 32' 11.248"
CAB-130	Agua Blanca Creek	Aguachica	Umir (Lower)	Early Campanian	8° 13' 25.725"	73° 32' 11.306"
CES-00	El Salto Creek	Aguachica	La Luna	Turonian to Santonian	8° 12' 08.312"	73° 31' 18.000"
CES-82	El Salto Creek	Aguachica	La Luna	Turonian to Santonian	8° 12' 05.444"	73° 31' 20.457"
CES1-00	El Salto Creek	Aguachica	La Luna	Turonian to Santonian	8° 12' 08.911"	73° 31' 13.229"
CES1-20	El Salto Creek	Aguachica	La Luna	Turonian to Santonian	8° 12' 08.853"	73° 31' 13.827"
GA-00	Gachalá	CEOR	Macanal	Berriasian – early Hauterivian	4° 41' 44.416"	73° 29' 43.044"
GA-62	Gachalá	CEOR	Macanal	Berriasian – early Hauterivian	4° 41' 45.454"	73° 29' 46.375"
MSP-00	M. San Pedro	CEOR	Macanal	Berriasian – early Hauterivian	4° 51' 23.858"	73° 22' 28.851"
MSP-36	M. San Pedro	CEOR	Macanal	Berriasian – early Hauterivian	4° 51' 24.804"	73° 22' 30.268"
O-00	Otanche	CEOC	Hilo	Middle and late Albian	5° 42' 50.420"	74° 11' 54.956"
O-96	Otanche	CEOC	Hilo	Middle and late Albian	5° 42' 49.222"	74° 11' 51.865"
QAD-00	Aguadulce Creek	Barichara	La Luna	Turonian to Santonian	7° 11' 06.173"	73° 17' 40.617"
QAD-77	Aguadulce Creek	Barichara	La Luna	Turonian to Santonian	7° 11' 06.670"	73° 17' 43.550"
QAD1-00	Aguadulce Creek 1	Barichara	La Luna	Turonian to Santonian	7° 11' 18.134"	73° 17' 32.182"
QAD1-60	Aguadulce Creek 1	Barichara	La Luna	Turonian to Santonian	7° 11' 18.037"	73° 17' 34.405"
QBB-00	Buriburi Creek	CEOC	Furatena (Lower)	Berriasian – early Hauterivian	5° 40' 36.746"	74° 03' 41.176"
QBB-12	Buriburi Creek	CEOC	Furatena (Lower)	Berriasian – early Hauterivian	5° 40' 36.717"	74° 03' 40.604"
QC-00	Cobre Creek	CEOC	Lidita Inferior	Late Santonian	5° 41' 41.386"	74° 12' 27.255"
QC-50	Cobre Creek	CEOC	Lidita Inferior	Late Santonian	5° 41' 39.970"	74° 12' 26.572"
QC1-00	Cobre Creek 1	CEOC	Lomagorda	Turonian to Santonian	5° 42' 04.020"	74° 12' 27.205"
QC1-54	Cobre Creek 1	CEOC	Lomagorda	Turonian to Santonian	5° 42' 02.266"	74° 12' 25.176"
QED-00	El Dátil Creek	CEOR	Fómeque	Barremian and Aptian	5° 01' 54.296"	73° 20' 25.292"
QED-36	El Dátil Creek	CEOR	Fómeque	Barremian and Aptian	5° 01' 55.929"	73° 20' 24.462"
QG-00	Guate Creek	Villeta	Lidita Inf.	Late Santonian	4° 53' 59.292"	74° 32' 03.307"
QG-137	Guate Creek	Villeta	Lidita Inf.	Late Santonian	4° 54' 01.026"	74° 32' 08.472"
QG-251	Guate Creek	Villeta	Lidita Sup.	Late Campanian	4° 54' 00.408"	74° 32' 13.807"
QG-292	Guate Creek	Villeta	Lidita Sup.	Late Campanian	4° 54' 00.354"	74° 32' 15.777"
QLL-00	La Leche Creek	Catatumbo	Guayacán	Cenomanian	8° 08' 56.797"	72° 41' 31.315"
QLL-02	La Leche Creek	Catatumbo	Guayacán	Cenomanian	8° 08' 57.311"	72° 41' 30.412"
QLL-04	La Leche Creek	Catatumbo	La Luna	Turonian to Santonian	8° 08' 57.822"	72° 41' 29.509"
QLL-63	La Leche Creek	Catatumbo	La Luna	Turonian to Santonian	8° 09' 09.873"	72° 41' 14.692"
QLM-00	Los Micos Creek	CEOR	Fómeque	Barremian and Aptian	5° 04' 22.882"	73° 24' 53.983"
QLM-53	Los Micos Creek	CEOR	Fómeque	Barremian and Aptian	5° 04' 20.588"	73° 24' 57.524"
QLP-00	La Paja Creek	Barichara	Paja	Barremian and Aptian	7° 01' 26.468"	73° 20' 04.444"
QLP-66	La Paja Creek	Barichara	Paja	Barremian and Aptian	7° 01' 25.114"	73° 20' 08.359"
QN-00	Negra Creek	CEOC	Villa de Leyva	Late Hauterivian	5° 35' 40.402"	73° 30' 02.088"

Table 1. Location of field sections (*continued*).

Sample	Section	Area	Formation	Age	Latitude N	Longitude W
QN-10	Negra Creek	CEOC	Villa de Leyva	Late Hauterivian	5° 35' 39.696"	73° 30' 02.193"
QNP-00	Negra Creek	CEOC	Paja	Barremian and Aptian	5° 35' 38.593"	73° 29' 56.222"
QNP-34	Negra Creek	CEOC	Paja	Barremian and Aptian	5° 35' 37.967"	73° 29' 54.923"
QP-00	Piñal Creek	Villeta	Hilo	Middle and late Albian	4° 52' 25.191"	74° 30' 09.671"
QP-465	Piñal Creek	Villeta	Hilo	Middle and late Albian	4° 52' 06.673"	74° 29' 55.123"
QS-00	La Sorda Creek	Barichara	El Salto	Cenomanian	7° 09' 38.294"	73° 18' 05.373"
QS-16	La Sorda Creek	Barichara	El Salto	Cenomanian	7° 09' 38.753"	73° 18' 05.597"
QS1-02	La Sorda Creek 1	Barichara	La Luna (Lower)	Turonian	7° 09' 50.411"	73° 18' 04.775"
QS1-36	La Sorda Creek 1	Barichara	La Luna (Lower)	Turonian	7° 09' 48.200"	73° 18' 06.301"
QS2-00	La Sorda Creek 2	Barichara	El Salto	Cenomanian	7° 09' 57.080"	73° 18' 00.931"
QS2-20	La Sorda Creek 2	Barichara	El Salto	Cenomanian	7° 09' 58.418"	73° 18' 01.340"
QS2-22	La Sorda Creek 2	Barichara	La Luna (Lower)	Turonian	7° 09' 58.552"	73° 18' 01.379"
QS2-52	La Sorda Creek 2	Barichara	La Luna (Lower)	Turonian	7° 10' 00.565"	73° 18' 01.991"
QSA-00	San Antonio Creek	CEOR	Aguacaliente	Late Campanian	4° 50' 15.031"	73° 12' 25.203"
QSA-100	San Antonio Creek	CEOR	Aguacaliente	Late Campanian	4° 50' 11.838"	73° 12' 25.178"
QSAC-00	S. Antonio Creek C	CEOR	Chipaque	Turonian to Santonian	4° 50' 34.658"	73° 12' 23.685"
QSAC-48	S. Antonio Creek C	CEOR	Chipaque	Turonian to Santonian	4° 50' 33.001"	73° 12' 23.408"
QSACH-00	S. Antonio Creek Ch	CEOR	Chipaque	Turonian to Santonian	4° 50' 27.921"	73° 12' 24.635"
QSACH-30	S. Antonio Creek Ch	CEOR	Chipaque	Turonian to Santonian	4° 50' 26.784"	73° 12' 24.231"
QSAU-00	S. Antonio Creek U	CEOR	Une (Upper)	Late Cenomanian	4° 51' 13.714"	73° 12' 14.776"
QSAU-18	S. Antonio Creek U	CEOR	Une (Upper)	Late Cenomanian	4° 51' 13.752"	73° 12' 14.292"
RC-00	Contador River	Villeta	Hilo (Lower)	Middle Albian	4° 52' 59.887"	74° 31' 09.813"
RC-44	Contador River	Villeta	Hilo (Lower)	Middle Albian	4° 52' 59.100"	74° 31' 08.615"
RCA-00	Cañas River	Villeta	Conejo	Turonian to Santonian	4° 56' 31.704"	74° 16' 10.733"
RCA-80	Cañas River	Villeta	Conejo	Turonian to Santonian	4° 56' 28.080"	74° 16' 02.777"
RN-00	Negro River	CEOC	Pacho	Cenomanian	5° 17' 35.949"	74° 04' 43.213"
RN-112	Negro River	CEOC	Pacho	Cenomanian	5° 17' 33.238"	74° 04' 52.281"
RR-02	Riecito River	Catatumbo	Capacho	Middle and late Albian	8° 03' 02.089"	72° 48' 26.230"
RR-20	Riecito River	Catatumbo	Capacho	Middle and late Albian	8° 03' 05.512"	72° 48' 26.056"
RR1-00	Riecito River 1	Catatumbo	Guayacán	Cenomanian	8° 03' 30.022"	72° 48' 26.355"
RR1-10	Riecito River 1	Catatumbo	Guayacán	Cenomanian	8° 03' 30.158"	72° 48' 27.350"
RR1-18	Riecito River 1	Catatumbo	La Luna	Turonian to Santonian	8° 03' 30.265"	72° 48' 28.150"
RR1-60	Riecito River 1	Catatumbo	La Luna	Turonian to Santonian	8° 03' 30.834"	72° 48' 32.337"
RSP-00	Samacá River	CEOC	Villa de Leyva	Late Hauterivian	5° 35' 19.005"	73° 30' 44.572"
RSP-32	Samacá River	CEOC	Villa de Leyva	Late Hauterivian	5° 35' 17.562"	73° 30' 43.650"
RSR-00	Samacá River	CEOC	Ritoque	Late Valanginian – early Hauterivian	5° 35' 30.385"	73° 30' 54.584"
RSR-34	Samacá River	CEOC	Ritoque	Late Valanginian – early Hauterivian	5° 35' 31.205"	73° 30' 51.049"
RT-00	Tobia River	Villeta	Murca (Lower)	Berriasian – early Hauterivian	5° 04' 16.218"	74° 26' 44.287"
RT-62	Tobia River	Villeta	Murca (Lower)	Berriasian – early Hauterivian	5° 04' 14.781"	74° 26' 40.134"
VV-00	Caiquero	Villeta	Trincheras	Barremian and Aptian	5° 03' 51.475"	74° 24' 41.054"
VV-89	Caiquero	Villeta	Trincheras	Barremian and Aptian	5° 03' 47.484"	74° 24' 32.936"

Table 2. Location of wells.

Sample	Well	Area	Formation	Age	Latitude N	Longitude W
CON-06-360	ANH-CON-06	CEOC	Churuvita	Cenomanian	5° 44' 26.202"	73° 44' 14.826"
CON-06-1470	ANH-CON-06	CEOC	Churuvita	Cenomanian	5° 44' 26.202"	73° 44' 14.826"
CON-07-134	ANH-CON-07	CEOC	Churuvita	Cenomanian	5° 49' 30.758"	73° 41' 47.587"
CON-07-240	ANH-CON-07	CEOC	Churuvita	Cenomanian	5° 49' 30.758"	73° 41' 47.587"
CON-07-485	ANH-CON-07	CEOC	San Gil Shale	Middle and late Albian	5° 49' 30.758"	73° 41' 47.587"
CON-07-1810	ANH-CON-07	CEOC	San Gil Shale	Middle and late Albian	5° 49' 30.758"	73° 41' 47.587"
CON-07-1880	ANH-CON-07	CEOC	San Gil Sandstone	Early Albian	5° 49' 30.758"	73° 41' 47.587"
CON-07-2420	ANH-CON-07	CEOC	San Gil Sandstone	Early Albian	5° 49' 30.758"	73° 41' 47.587"
CON-08-287	ANH-CON-08	CEOC	San Gil Sandstone	Early Albian	5° 57' 12.630"	73° 36' 31.512"
CON-08-1310	ANH-CON-08	CEOC	San Gil Sandstone	Early Albian	5° 57' 12.630"	73° 36' 31.512"
CON-08-1376	ANH-CON-08	CEOC	Paja	Barremian and Aptian	5° 57' 12.630"	73° 36' 31.512"
CON-08-2575	ANH-CON-08	CEOC	Paja	Barremian and Aptian	5° 57' 12.630"	73° 36' 31.512"
COS-05-261	ANH-COS-05	Villa de Leyva	Conejo	Turonian to Santonian	5° 31' 54.705"	73° 49' 49.929"
COS-05-1059	ANH-COS-05	Villa de Leyva	Conejo	Turonian to Santonian	5° 31' 54.705"	73° 49' 49.929"
COS-14-370	ANH-COS-14	Villa de Leyva	Villa de Leyva	Late Hauterivian	5° 35' 01.356"	73° 31' 30.586"
COS-14-650	ANH-COS-14	Villa de Leyva	Villa de Leyva	Late Hauterivian	5° 35' 01.356"	73° 31' 30.586"
COS-14-678	ANH-COS-14	Villa de Leyva	Ritoque	Late Valanginian – early Hauterivian	5° 35' 01.356"	73° 31' 30.586"
COS-14-1506	ANH-COS-14	Villa de Leyva	Ritoque	Late Valanginian – early Hauterivian	5° 35' 01.356"	73° 31' 30.586"
COS-15-893	ANH-COS-15	Villa de Leyva	San Gil Sandstone	Early Albian	5° 32' 37.037"	73° 38' 06.689"
COS-15-1323	ANH-COS-15	Villa de Leyva	San Gil Sandstone	Early Albian	5° 32' 37.037"	73° 38' 06.689"
COS-15-1330	ANH-COS-15	Villa de Leyva	Paja	Barremian and Aptian	5° 32' 37.037"	73° 38' 06.689"
COS-15-2220	ANH-COS-15	Villa de Leyva	Paja	Barremian and Aptian	5° 32' 37.037"	73° 38' 06.689"
INFA-4727	Infantas-1613	MMV	La Luna	Turonian to Santonian	6° 55' 38.423"	73° 46' 43.388"
INFA-6243	Infantas-1613	MMV	La Luna	Turonian to Santonian	6° 55' 38.423"	73° 46' 43.388"
INFA-6396	Infantas-1613	MMV	El Salto	Cenomanian	6° 55' 38.423"	73° 46' 43.388"
INFA-6472	Infantas-1613	MMV	El Salto	Cenomanian	6° 55' 38.423"	73° 46' 43.388"
INFA-6480	Infantas-1613	MMV	Simití	Middle and late Albian	6° 55' 38.423"	73° 46' 43.388"
INFA-8840	Infantas-1613	MMV	Simití	Middle and late Albian	6° 55' 38.423"	73° 46' 43.388"
INFA-8650	Infantas-1613	MMV	Tablazo	Early Albian	6° 55' 38.423"	73° 46' 43.388"
INFA-9358	Infantas-1613	MMV	Paja	Barremian and Aptian	6° 55' 38.423"	73° 46' 43.388"
INFA-9364	Infantas-1613	MMV	Paja	Barremian and Aptian	6° 55' 38.423"	73° 46' 43.388"
RIO-3496	Río de oro-14	Catatumbo	Mito Juan	Early Maastrichtian	9° 05' 37.499"	72° 54' 04.926"
RIO-4220	Río de oro-14	Catatumbo	Mito Juan	Early Maastrichtian	9° 05' 37.499"	72° 54' 04.926"
RIO-4780	Río de oro-14	Catatumbo	Colón (Lower)	Early Campanian	9° 05' 37.499"	72° 54' 04.926"
RIO-5392	Río de oro-14	Catatumbo	Colón (Lower)	Early Campanian	9° 05' 37.499"	72° 54' 04.926"
RIO-5768	Río de oro-14	Catatumbo	La Luna	Turonian to Santonian	9° 05' 37.499"	72° 54' 04.926"
RIO-5775	Río de oro-14	Catatumbo	La Luna	Turonian to Santonian	9° 05' 37.499"	72° 54' 04.926"
RIO-6259	Río de oro-14	Catatumbo	Capacho	Middle and late Albian	9° 05' 37.499"	72° 54' 04.926"
SAR-7336	Sardinata-n2	Catatumbo	La Luna	Turonian to Santonian	8° 30' 15.474"	72° 39' 04.879"
SAR-7460	Sardinata-n2	Catatumbo	La Luna	Turonian to Santonian	8° 30' 15.474"	72° 39' 04.879"

sponds to La Luna Formation in the Aguachica area; the lowest content (0.2% TOC) is from the Ritoque Formation in the Villa de Leyva area.

Thermal maturity values are derived from vitrinite reflectance and pyrolysis. The limestones include Ro data that have at least 10 particles of vitrinite per sample. The shales include Ro data that have at least 40 particles of vitrinite per sample. Thermal maturity from pyrolysis comes from reliable Tmax values from samples with more than 0.2 mg HC/g at S2.

The Ro values from La Luna Formation are in the oil and early gas generation windows (0.8–1.3 % Ro). The highest thermal maturity values obtained from pyrolysis are from the Upper Cretaceous Oliní Group (2.4–2.8 % Ro) and Conejo Formation (2.9% Ro). The highest thermal maturity values obtained from vitrinite are from the Lower Cretaceous Murca, Trincheras, and Hilo Formations from the Villeta area (4.0–4.2 % Ro) and the Paja Formation from the Villa de Leyva area (4.3% Ro).

Table 4 shows the average values of gas collected in the 200 canister samples cored from field exposures, along with the TOC average values per section. The samples with the highest TOC and gas contents in the upper part of the table are from La Luna, Guayacán, Hilo, and Paja Formations. The values correspond to total gas, which includes lost and desorbed gas before fracturing and grinding the rock and residual gas after these procedures. Total gas includes hydrocarbons, CO₂, nitrogen, and oxygen. The results are ordered by gas content.

Table 5 displays the gas chromatography results with the best sample of each section in terms of the highest contents of gaseous hydrocarbons released in the 200 canister tests, along with the averages of TOC and Ro per section. The table includes the contents of the most abundant gases, including methane, ethane, and propane. The results are ordered by the total percentage of gas hydrocarbons; the highest ones are in the upper part of the table and correspond to La Luna, Lidita Inferior, Lidita Superior, Hilo, Guayacán, and Paja Formations.

Table 6 presents the samples with the highest volumes of hydrocarbons, along with the residual versus desorbed gas ratio and the CO₂ content. The results from a total of 200 samples are ordered by hydrocarbon percentage. The highest values in the upper part of the table correspond to La Luna, Lidita Inferior, Lidita Superior, Hilo, Guayacán, and Paja Formations.

Table 7 shows the porosity and permeability average values per section, along with the average gas hydrocarbon content. The results from a total of 500 samples are ordered by porosity values; the lowest ones are in the upper part of the table and correspond to the units with the highest hydrocarbon content.

Table 8 displays the pyrolysis results, along with the TOC and thermal maturity values per section. The samples are ordered by the average content of hydrocarbons released at the S2 peak. The TOC averages included in the table are those of the 500 samples processed for pyrolysis and are in general higher than those compiled in Table 3, which correspond to

the total 1500 samples of the study. This is because the samples with higher TOC from each section were chosen for the pyrolysis analysis.

4. Discussion

4.1. TOC and Thermal Maturity

The best values of TOC and thermal maturity are found in the biomicrites and diagenetic cherts of La Luna Formation, the Hilo Formation, and the Oliní Group, from the N and W sides of the basin (Figures 4–7; Tables 3–5).

The Ro values obtained from vitrinite reflectance and pyrolysis data (Figures 6, 7; Table 3) are present in two lithological groups, calcareous and terrigenous, which have very different properties in terms of maturity and TOC contents. Because the particles of vitrinite are of terrigenous origin, the rocks that contain more analyzed points and yield more reliable results are the mudstones and shales that have higher contents of clay minerals and organic matter of terrestrial origin. In this shale (and marlstone) group, the San Gil Superior Shale from well CON–7 and the Paja Formation from wells CON–8 and COS–15 are notable because they have between 40 and 70 vitrinite particles analyzed.

The biomicrites, as well as the biosparites and siltstones with low amounts of terrigenous mud, are placed in the other group, with very few or no particles of vitrinite. The most notable rocks of this group are the foraminiferal biomicrites of La Luna Formation, which have very few particles, usually 1 or 2 per sample, and do not produce reliable average Ro results. In these rocks, the pyrolysis results yield a better approximation of thermal maturity. The biomicrites of the Hilo and Lomagorda Formations, along with the Oliní Group, also have very few vitrinite particles, approximately 3 to 6 on average. For instance, there is a huge difference between the vitrinite (0.8% Ro) and pyrolysis (2.4–2.8 % Ro) values of the Oliní Group due to the scarcity of vitrinite particles. A few siltstones, muddy sandstones, and biosparites interbedded in the Ritoque (well COS–14), Churuvita (well CON–6), and Conejo Formations (well COS–5) are also good examples of nonreliable thermal maturity values from vitrinite.

The best TOC results are those of La Luna Formation biomicrite (Turonian to Santonian TST and HST), which has averages per section between 4.9 and 11.6% TOC. These averages are even higher than the 4–8 % TOC averages compiled by Kennedy et al. (2016) from the prolific Eagle Ford biomicrite of Texas, which has the same age as La Luna Formation and is currently producing nonconventional oil and gas. Very high individual values were obtained from samples at caño El Salto (CES–1) from Aguachica (21.7% TOC), Aguadulce Creek (QAD) from the W foothills of the Eastern Cordillera (18.2% TOC), and caño Aguablanca (CAB) also from Aguachica

Table 3. TOC vs. Thermal maturity.

Formation	Alloformation age	Stratigraphic section	Area	TOC average (%)	Ro average (%) Vitrin – Pyrol
La Luna	Turonian to Santonian	CES1	Aguachica	11.6	PYR 0.8
Guayacán	Cenomanian	QLL	Catatumbo	8.7	PYR 1.2
La Luna	Turonian to Santonian	CES	Aguachica	8.6	PYR 0.8
La Luna	Turonian to Santonian	QS2	Barichara	8.6	PYR 0.9
La Luna	Turonian to Santonian	RIO-14	Catatumbo	8.1	VIT 0.3 PYR 1.0
La Luna	Turonian to Santonian	SAR-N2	Catatumbo	7.7	VIT 1.0 PYR 1.3
La Luna	Turonian to Santonian	RR1	Catatumbo	7.2	VIT 0.8 PYR 1.1
La Luna	Turonian to Santonian	QS1	Barichara	7	VIT 0.4 PYR 0.9
La Luna	Turonian to Santonian	QAD1	Barichara	6.5	VIT 0.4 PYR 0.8
La Luna	Turonian to Santonian	QLL	Catatumbo	6.1	VIT 0.6 PYR 1.2
Hilo	Middle and late Albian	QP	Villeta	5.8	VIT 4.0
Paja	Barremian and Aptian	QNP	Villa de Leyva	5.8	VIT 3.1
La Luna	Turonian to Santonian	INFAN-1613	Middle Magdalena Valley	5.6	PYR 0.9
La Luna	Turonian to Santonian	QAD	Barichara	5.4	VIT 0.4 PYR 0.8
Furatena (lower section)	Berriasian to early Hauterivian	QBB	W Emerald B	5.3	VIT 3.1
Hilo	Middle and late Albian	O	W Emerald B	5.3	VIT 3.5
Hilo	Middle and late Albian	RC	Villeta	4.9	VIT 3.4
La Luna	Turonian to Santonian	CAB	Aguachica	4.9	PYR 0.8
Lomagorda	Turonian to Santonian	QC1	UMV-W Foothills	4.5	VIT 2.4
Furatena (lower section)	Berriasian to early Hauterivian	BB	W Emerald B	4.4	VIT 3.1
Paja	Barremian and Aptian	QLP	Barichara	3.8	PYR 1.9
Guayacán	Cenomanian	RR1	Catatumbo	3.7	PYR 1.1
Trincheras	Barremian and Aptian	VV	Villeta	3.5	VIT 4.0
Lidita Superior	Late Campanian	QG	UMV-Villeta	3.1	VIT 0.8 PYR 2.4
Lidita Inferior	Late Santonian	QC	UMV-W Foothills	3	VIT 2.4
Lidita Inferior	Late Santonian	QG	UMV-Villeta	2.7	VIT 0.8 PYR 2.8
Paja	Barremian and Aptian	CON-8	Villa de Leyva	2.7	VIT 3.1
El Salto	Cenomanian	QS2	Barichara	2.4	PYR 0.9
San Gil Sandstone	Early Albian	CON-8	Villa de Leyva	2.4	VIT 2.5
Paja	Barremian and Aptian	COS-15	Villa de Leyva	2.3	VIT 4.3
Macanal	Berriasian to early Hauterivian	GA	E Emerald B	2.1	VIT 3.7
San Gil Sandstone	Early Albian	COS-15	Villa de Leyva	1.9	VIT 3.8
Villa de Leyva	Late Hauterivian	COS-14	Villa de Leyva	1.8	VIT 3.4
Conejo	Turonian to Santonian	COS-5	Villa de Leyva	1.7	VIT 2.9
Conejo	Turonian to Santonian	RCA	Villeta	1.6	PYR 2.9
Murca (lower Section)	Berriasian to early Hauterivian	RT	Villeta	1.4	VIT 4.2
San Gil Shale	Middle and late Albian	CON-7	Villa de Leyva	1.4	VIT 2.6
San Gil Sandstone	Early Albian	CON-7	Villa de Leyva	1.2	VIT 3.2
El Salto	Cenomanian	QS	Barichara	1.1	PYR 0.9
Capacho	Middle and late Albian	RR	Catatumbo	0.8	PYR 1.2
Churuvita	Cenomanian	CON-7	Villa de Leyva	0.7	VIT 2.5
Chipaque	Turonian to Santonian	QSACH	Llanos Foothills	0.6	PYR 0.6
Une (upper section)	Cenomanian	QSAU	Llanos Foothills	0.6	PYR 0.9
Chipaque	Turonian to Santonian	QSAC	Llanos Foothills	0.5	PYR 0.6
Churuvita	Cenomanian	CON-6	Villa de Leyva	0.5	VIT 2.2
Aguacaliente	Late Campanian	QSA	Llanos Foothills	0.4	PYR 0.6
Ritoque	Berriasian to early Hauterivian	COS-14	Villa de Leyva	0.2	VIT 3.9

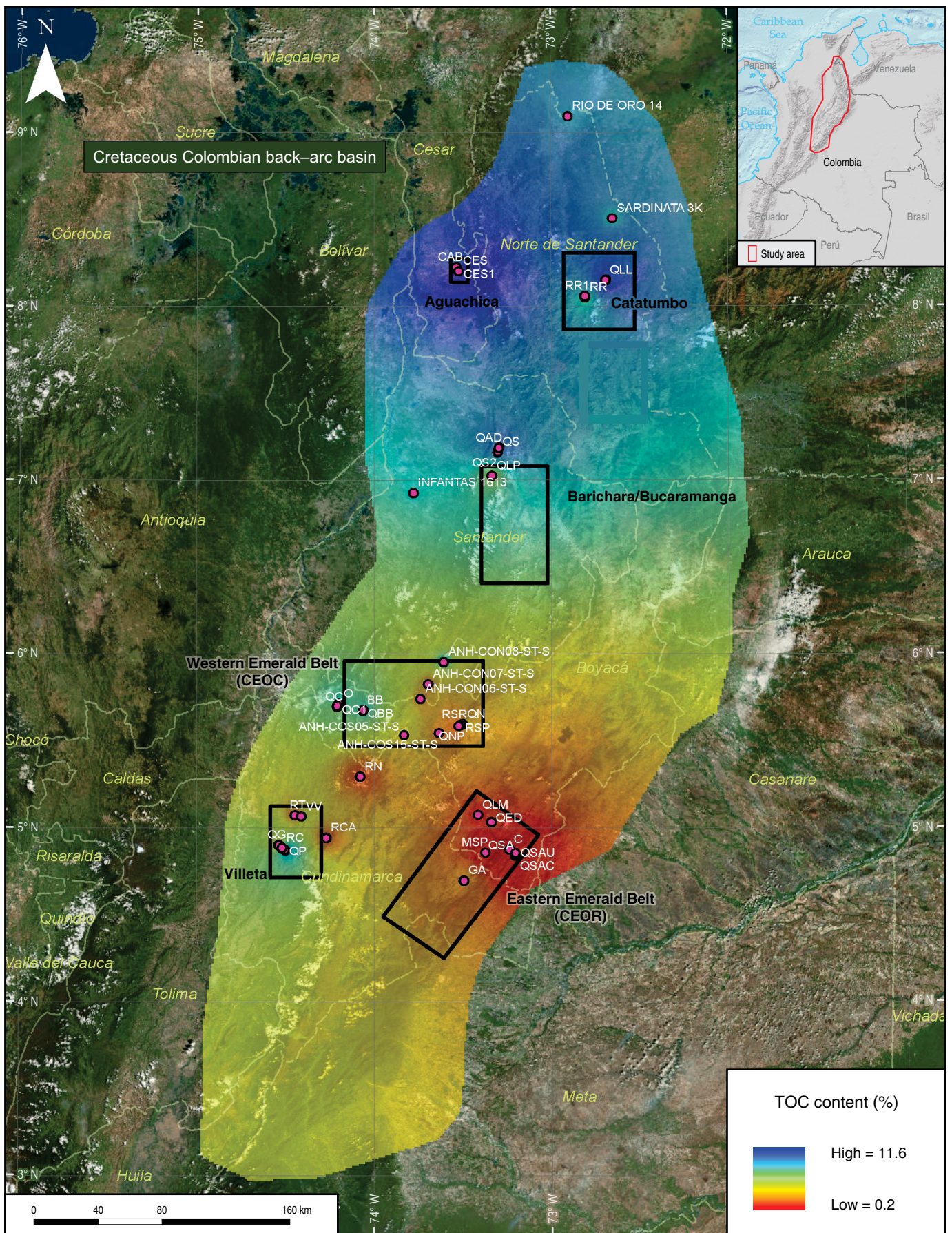
Table 4. Gas content vs. TOC.

Formation	Alloformation Age	Stratigraphic Section	Area	Total Gas (feet ³ /ton)	TOC (%)
Guayacán	Cenomanian	RR1	Catatumbo	16.18	3.7
La Luna	Turonian to Santonian	QS2	Barichara	15.63	8.6
La Luna	Turonian to Santonian	RR1	Catatumbo	14.59	7.2
Murca (lower section)	Berriasian to early Hauterivian	RT	Villeta	14.42	1.4
Capacho	Middle and late Albian	RR	Catatumbo	13.74	0.8
Furatena (lower section)	Berriasian to early Hauterivian	BB	W Emerald B	13.68	4.4
La Luna	Turonian to Santonian	CAB	Aguachica	13.51	4.9
El Salto	Cenomanian	QS2	Barichara	13.01	2.4
Paja	Barremian and Aptian	QLP	Barichara	12.89	3.8
Lidita Inferior	Late Santonian	QC	UMV–W foothills	12.51	3
La Luna	Turonian to Santonian	CES1	Aguachica	12.04	11.6
Hilo	Middle and late Albian	O	W Emerald B	11.84	5.3
La Luna	Turonian to Santonian	QAD1	Barichara	11.67	6.5
Une (upper section)	Cenomanian	QSAU	Llanos Foothills	11.63	0.6
La Luna	Turonian to Santonian	CES	Aguachica	11.59	8.6
Villa de Leyva	Late Hauterivian	RSP	Villa de Leyva	11.48	1.3
Macanal	Berriasian to early Hauterivian	GA	E Emerald B	10.9	2.1
La Luna	Turonian to Santonian	QS1	Barichara	10.3	7
Chipaque	Turonian to Santonian	QSACH	Llanos Foothills	9.91	0.6
La Luna	Turonian to Santonian	QAD	Barichara	9.1	5.4
La Luna	Turonian to Santonian	QLL	Catatumbo	9.02	6.1
Macanal	Berriasian to early Hauterivian	C	E Emerald B	8.89	1.4
Aguacaliente	Late Campanian	QSA	Llanos Foothills	8.5	0.4
Hilo	Middle and late Albian	QP	Villeta	8.47	5.8
Chipaque	Turonian to Santonian	QSAC	Llanos Foothills	7.8	0.5
Ritoque	Berriasian to early Hauterivian	RSR	Villa de Leyva	7.79	0.6
Trincheras	Barremian and Aptian	VV	Villeta	7.67	3.5
Fómeque	Barremian and Aptian	QLM	E Emerald B	7.43	1.1
Macanal	Berriasian to early Hauterivian	MSP	E Emerald B	7.34	0.6
Conejo	Turonian to Santonian	RCA	Villeta	7.33	1.6
Fómeque	Barremian and Aptian	QED	E Emerald B	6.93	1.4
Lidita Superior	Late Campanian	QG	UMV–Villeta	6.46	3.1
Hilo	Middle and late Albian	RC	Villeta	6.39	4.9
Guayacán	Cenomanian	QLL	Catatumbo	6.25	8.7
Lidita Inferior	Late Santonian	QG	UMV–Villeta	6.23	2.7
El Salto	Cenomanian	QS	Barichara	5.52	1.1
Villa de Leyva	Late Hauterivian	QN	Villa de Leyva	4.88	0.8
Paja	Barremian and Aptian	QNP	Villa de Leyva	4.78	5.8

(13.9% TOC). The Ro maturity values of La Luna Formation (from Tmax) are also excellent, between 0.8 and 1.3%, in the oil and early gas generation windows.

The TOC average percentages presented here from 212 samples of La Luna Formation, collected from 9 field sections

Figure 4. Distribution of average TOC values per section from 1500 samples. The highest percentages are on the N and W sides of the basin. 



and three wells (Table 3), are also higher than the 4.0% TOC documented by Liborius & Slatt (2014) from 20 data points from a well in the Maracaibo area of Venezuela and higher than the values of 4.3% TOC (Zumberge, 1984) and 4.0% TOC (Casadiego & Rios, 2016) from exposures W of Bucaramanga. Torres *et al.* (2015) also reported values as high as 11.9% TOC from an area W of Bucaramanga, but the average of 34 data points appears to be approximately 2.5% TOC. Galvis–Portilla *et al.* (2014) reported TOC data from a 120–feet interval of a well in the Middle Magdalena Valley (MMV), with 11 values between 1.3 and 5.3% TOC and an average of approximately 3.0% TOC. Veiga & Dzelalija (2014) reported TOC values between 2 and 5% TOC with thermal maturity from 0.8–1.3 % Ro from Catatumbo and between 2 and 6% TOC with thermal maturity from 0.5–1.3 % Ro from the MMV, which match our maximum thermal maturity results but are below our TOC averages. Most of the TOC values from La Luna in the Catatumbo area compiled by Aguilera *et al.* (2010) are in the range of 4–6 % TOC, with 10 points between 6 and 8% TOC, which are within the range of the 6.1–8.1 % TOC averages presented here from 80 samples from the Cúcuta/Catatumbo area; most of their thermal maturity values are between 0.8 and 1.5% Ro. Aguilera *et al.* (2010) also compiled data from the MMV, showing that most TOC data points are between 2 and 4% TOC, with 7 samples between 4 and 6% TOC, which are lower than the 4.9–11.6 % TOC averages presented here; most of their Ro values are between 0.6–0.9 % Ro with a few between 0.9–1.3 % Ro, which present a wider range than the 0.8–0.9 % Ro presented here for the MMV from 132 samples (Table 3).

Most of the Turonian to Santonian limestones of the basin, including La Luna and Lomagorda Formations, are biomicrites of planktonic foraminifera (Figure 5) deposited in a deep–sea offshore environment, between 150 and 200 m depths, and far from terrigenous sources. Centimeter–scale chert beds are present as a diagenetic transformation of these biomicrites. There are also minor amounts of impure biomicrites (10–35 % clay minerals and silt–sized quartz particles) and minor amounts of marlstones (a nearly equal mixture of calcareous and terrigenous mud particles), as indicated by the petrography, XRD, and ICP–MS chemical analysis (Guerrero *et al.*, 2000, 2020). In general, the Lomagorda and La Luna Formations have very little contribution of terrigenous material, including clay minerals, silt–sized quartz particles, and vitrinite particles.

Other rock names, such as “fossiliferous claystone”, “siliceous claystone”, “calcareous claystone”, “fossiliferous shale”, “siliceous shale”, “calcareous shale”, “argillaceous limestone”, “siliceous mudstone”, “argillaceous mudstone”, “calcareous mudstone”, and so on, have been inaccurately used for La Luna Formation and are either the result of inappropriate rock classification or misidentification of the unit.

In the first case, concerning inappropriate rock classification, the dark–colored, organic–rich calcareous mud matrix

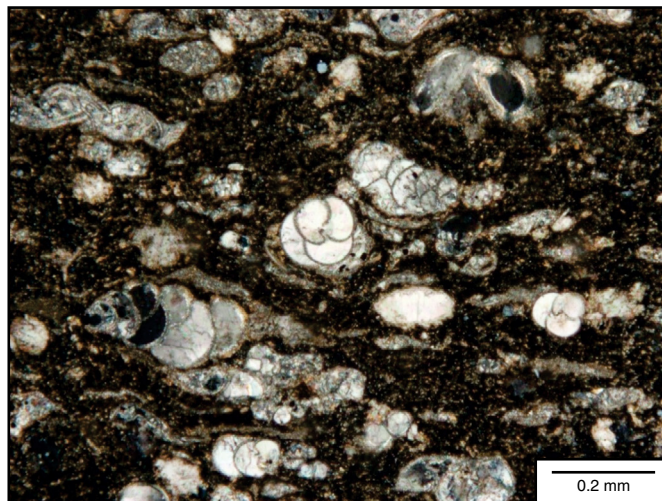


Figure 5. Thin section photograph of a silicified biomicrite (sample QAD–20) from La Luna Formation at the Aguadulce Creek W of Bucaramanga. Large foraminifera have a length of 100 to 200 μm . The matrix is composed of organic matter and quartz–replaced calcareous mud (silt– and clay–sized fragments of foraminifera and calcareous algae). The sample contains 5% terrigenous mud (clay minerals and silt–sized quartz particles), 60% diagenetic quartz, and 35% calcite.

(fragments of foraminifera, calcareous algae, and coccoliths), and the diagenetically silicified chert matrix, are erroneously identified as terrigenous claystones and/or mudstone shales, although in those rocks, the only observable framework particles in the petrographic microscope are foraminifera, fish bones, and fecal pellets in the range of coarse silt and sand–sized bioclasts. The petrography and the chemical ICP–MS and XRD analysis of these rocks indicate a dominance of calcite and quartz (diagenetic quartz instead of terrigenous quartz), with very little or no clay minerals.

In the second case, concerning the misidentification of the unit, the shale beds of the upper part of the Simití Formation were erroneously included in the “salada” and “pujamana” members of La Luna Formation at a proposed type locality (Morales *et al.*, 1958) W of Bucaramanga, where La Luna biomicrite and the Simití shale are in faulted contact. Since then, researchers have tried to identify three members in La Luna Formation, creating difficulties in the identification of the unit and major correlation problems; for example, Casadiego & Rios (2016) indicated that the “pujamana” member of other authors corresponds to the “galembó” member at the Agua–blanca section W of Bucaramanga. The enormous thickness of approximately 3000 feet from cores reported by Galvis–Portilla *et al.* (2014) also suggests that the authors may have included strata from more than one unit in their definition of La Luna Formation. The thickness of the Turonian to Santonian limestones exposed at the type locality of La Luna Formation in Venezuela and in the rest of the basin in Colombia (Guerrero,

2002b) reaches a maximum measured thickness of 700 to 900 feet, so it is difficult to believe that the unit could reach 2500 to 3000 feet in oil wells.

Other rocks laterally adjacent (on the same Turonian to Santonian TST and HST facies belts) have maturity data slightly lower in the early oil generation window, such as the Chipaque Formation shales of the Llanos Foothills (0.6% Ro), but very low contents of organic matter (0.5–0.6 % TOC).

The Conejo Formation, which is located closer to the center of the basin than the Chipaque Formation, has much higher thermal maturity, between 2.6 and 2.9% Ro (well COS–5), in the late generation gas window, with TOC values between 1.6 and 1.7%, which are also somewhat low. However, one sample from La Frontera Member in the lower part of the Conejo Formation at the COS–5 well had the highest TOC (24.8%) of the whole study.

Toward the west, the Lomagorda Formation from the Cobre Creek (QC1) in the W foothills of the Eastern Cordillera has maturity values of approximately 2.4% Ro, which are also in the late generation gas window, but has average values of TOC (4.5%) comparable with the lowest values of La Luna Formation. The highest content from the Lomagorda Formation in the study area was 7.4% TOC. Veiga & Dzelalija (2014) reported TOC values from 5 wells of the Lomagorda Formation in the UMV (they used the name “la luna”) of between 1.45 and 2.75% TOC. However, the enormous reported thicknesses in some wells (up to 2650 feet) and the absence of the Lidita Inferior and Lidita Superior of the Oliní Group introduces doubts regarding the identification of the units. Aguilera et al. (2010) compiled values between 1 and 9% TOC from the Lomagorda Formation of the UMV (they also used the name “la luna”) with immature organic matter showing values below 0.5% Ro.

The late Santonian Lidita Inferior Unit has essentially the same lithology as the Lomagorda Formation (biomicroites of planktonic foraminifera) but is partially replaced by diagenetic quartz (Guerrero et al., 2000) due to its proximity with the regressive terrigenous strata of Campanian age (middle part of the Oliní Group). The TOC average values of the Lidita Inferior are between 2.7 (QG) and 3.0% (QC); the highest TOC of the Lidita Inferior at the Cobre Creek was 6.8%.

The biomicroites, diagenetic cherts, marlstones, and shales of the middle and late Albian transgressive and high sea level intervals (Tetuán, Hilo, San Gil Superior, Simití, and Capacho) present significant differences in terms of TOC and Ro. The best TOC values correspond to the Hilo Formation, whose averages are very good and range from 4.9–5.8 % TOC, but the unit is apparently overmature, with Ro vitrinite values between 3.4 and 4.0%. The highest TOC of the Hilo Formation was 12.1% at the Otanche (O) section. The San Gil Superior Shale of well CON–7 is on the late gas generation window (2.6% Ro), but it has a low average value of TOC (1.4%). The Capacho Formation of the Catatumbo area is in the early gas generation

window (1.2% Ro) and has a low content of organic matter (0.8% TOC). Veiga & Dzelalija (2014) reported TOC values of the Tetuán Formation between 1.78 and 4.42% TOC from 5 wells of the UMV. Aguilera et al. (2010) also compiled abundant data between 2–10 % TOC and 0.5–0.8 % Ro from the Tetuán Formation.

Units of Barremian and Aptian transgressive and high sea levels (Paja, Fόμεque, and Trincheras Formations) have acceptable values for TOC, between 2.3 and 5.8% but are generally overmature, with values between 3.1 and 4.3% Ro in wells CON–8 and COS–15. There is, however, an interesting exception at the type locality of the Paja Formation in the W foothills of the Eastern Cordillera, where it has 3.8% TOC and 1.9% Ro, putting it in the gas generation window.

The oldest units of the succession, in the Berriasian to Hauterivian interval, are even more overmature, with 3.7% Ro in the Macanal Formation from Gachalá (GA), 4.2% Ro in the Murca Formation of the Tobia River (RT), 3.9% Ro in the Ritoque Formation from COS–14 well, and 3.4% Ro in the overlying Villa de Leyva Formation in the same well COS–14.

In general, biomicroites of foraminifera have much higher contents of TOC than shales, so that instead of gas shales, the gas biomicroites constitute a far better target. Because biomicroites have lower clay contents (down to zero) than claystone and mudstone shales, it is expected that the biomicroites have a more brittle behavior than shales during the process of fracking. In addition, the plastic behavior of the clay shales will more easily close the induced fractures than the brittle behavior of the biomicroite limestones.

Thermal maturity values in the oil and early gas windows are good in the E and W borders and very good in the N side of the basin, where it opened to the proto-Caribbean. The strata from the axis of the basin are thermally overmature, especially in the areas proximal to the gabbroic intrusions and associated hydrothermal activity, which increased the thermal gradient during the Berriasian to Cenomanian main extension of the back-arc basin (Guerrero et al., 2020).

4.2. Gas Content in Canister Samples

The volumes of gas released from 200 canister samples taken from field exposures are compared with the TOC and Ro values of several formations (Figures 8, 9; Tables 5, 6). Airtight cylindrical containers of metal (canisters) were used to collect and measure gases in drilled cores of approximately 1 foot in length and 1.6-inch diameter, taken at a depth of 3 m below the surface. Most of the units measured are from transgressive and high sea level (TST and HST) biomicroites, marlstones, and shales, with some exceptions in regressive sea level (RST) shale units.

Gas chromatography revealed the presence of methane, ethane, propane, isobutane, butane, neopentane, isopentane, pentane, and hexane. In most of the samples studied, methane

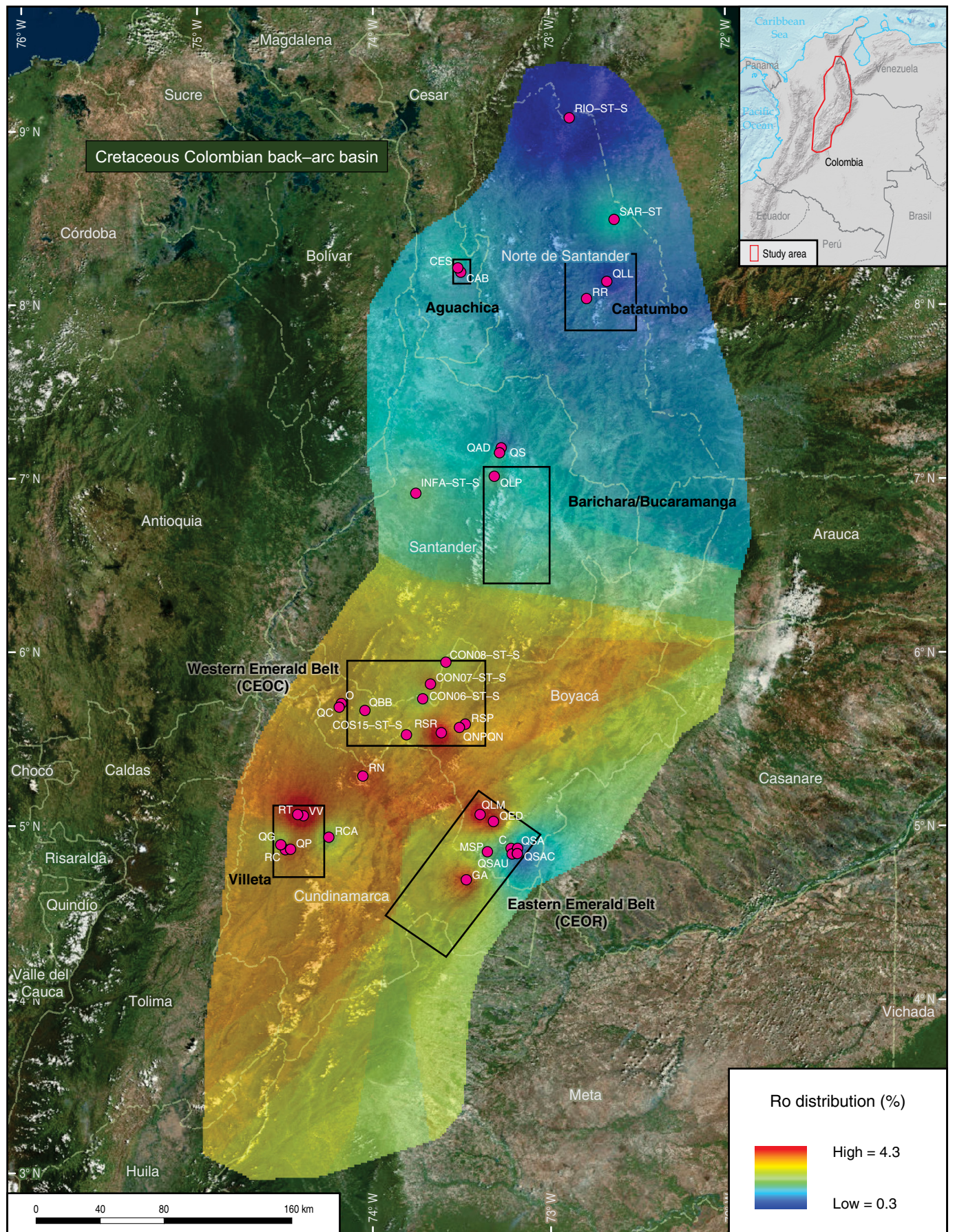




Figure 6. Distribution of thermal maturity (vitrinite reflectance) average values per section. The strata of the N area of the basin have lower thermal maturity than those of the central and SW areas. 1500 samples.

constitutes the main volume of gaseous hydrocarbons (Figures 9, 10; Table 5), followed by ethane and propane. All samples also contained a mixture of nitrogen and oxygen obtained from air exposure near the surface. This mixture varies between 19 and 91% of the total gases collected, so many samples had high contents of air instead of gaseous hydrocarbons; the samples with the highest air contamination (nitrogen and oxygen) were the shales of the Ritoque, Villa de Leyva, Paja, Macanal, Fόμεque, Chipaque, and Aguacaliente Formations. CO₂ was also present in significant volumes that reached 15.3%, with the highest percentages obtained in samples of the Conejo, El Salto, La Luna, Macanal, Fόμεque, Une, Chipaque, Aguacaliente, Murca, Trincheras, and Hilo Formations.

Samples with the lowest CO₂ contents (3.0–11.5 %) were associated with the highest hydrocarbon contents (15.0–77.8 %), which include the limestones and cherts of La Luna, Lidita Inferior, Lidita Superior, Hilo, Guayacán, and Paja Formations (Figure 11; Table 6). The results are important because although these rocks have lost important amounts of gas during uplift fracturing and have also been near the surface for some time, they still contain hydrocarbons stored in micropores and microfossil cavities.

Notably, gas contents are present in the biomicroites of La Luna Formation (TST and HST of the Turonian to Santonian time span), with average contents of total gas per section between 9.02 and 15.63 cubic feet per ton (feet³/ton). The best sample of the whole study (QLL-40 from La Leche Creek) released 5.10 feet³/ton of hydrocarbons, corresponding to 77.8% of its total gas content.

Additionally, in these areas, the TOC average values per section are excellent, ranging from 11.6% in El Salto Creek (CES1) in the Aguachica area, 8.6% in La Sorda Creek (QS2) in the Barichara area, and 7.2% in the Riecito River (RR1) in the Cúcuta area. In addition to the very high averages per section, individual samples have amazing organic carbon contents that range from 21.7 (sample CES1-02 from the Aguachica area) to 18.2% TOC (sample QAD-64 from the Barichara area) and 11.1% TOC (sample RR1-30 from the Cúcuta area).

In contrast, laterally adjacent units composed mainly of mudstone and shale have very low contents of gaseous hydrocarbons and TOC, such as the Chipaque Formation of the Llanos Foothills, which only reaches 0.5% TOC (QSAC) and 0.6% TOC (QSACH) in San Antonio Creek, with maximum hydrocarbon contents of 0.004% to 0.1%. The Conejo Formation at the Cañas River (RCA) in the Villeta area is slightly better, with a maximum 3.3% gaseous hydrocarbon content and TOC average of 1.6%. The three units belong to the same interval of time (Turonian to Santonian), constitute source rock

and still contain hydrocarbons, but the biomicroites of La Luna Formation are much richer in TOC and release more gaseous hydrocarbons than the shales of the other units. Therefore, La Luna Formation constitutes the most promising unit for unconventional hydrocarbons, not only because of its high content of gas and its very high content of TOC but also because the biomicroite limestones break better and maintain open fractures better than muddy units with high contents of clay minerals. The mudstones and shales do not break easily due to their plastic behavior, and the induced fractures close more quickly than in the biomicroites.

The Guayacán Formation (Cenomanian) from the Cúcuta area also presents high values of hydrocarbons and TOC. Total gaseous hydrocarbons comprise up to 27.2% of the gases measured (6.25 feet³/ton), with a TOC average of 8.7% (QLL). The highest TOC value (9.4%) of the unit is from sample RR1-02 at the Riecito River. The Guayacán Formation is a regressive unit (RST) that contains shales similar to those of the underlying Capacho Formation (TST and HST of the middle and late Albian) but differs by its content of minor interbedding of bivalve biosparites and arenites deposited in a progradational set of offshore to shoreface parasequences. The upper part of the Guayacán Formation can also serve as a conventional reservoir filled with hydrocarbons generated by the Capacho Formation and the lower part of the Guayacán Formation. The seal of this reservoir is made by the biomicroites and marlstones of La Luna Formation.

Other units that deserve special mention are the late Santonian to Campanian biomicroites and cherts of the Lidita Inferior and Lidita Superior of the Oliní Group from the Guate Creek (QG), west of the Bituima Fault. The highest gaseous hydrocarbon canister contents are between 34.3 and 37.3% of their total gas content (10.47 to 12.71 feet³/ton), with TOC values between 2.7 and 3.1%. The highest hydrocarbon contents from the Oliní Group were between 3.91 and 4.36 feet³/ton. The highest methane content of the whole study (4.35 feet³/ton) comes from sample QG-251 of the Lidita Superior (Figures 9, 10, 12; Table 5). The data of gas released from the Oliní Group are very important because the same units are present over a large area in the UMV, along with other thick biomicroite units, which include the Lomagorda (Turonian to Santonian) and Tetuán (middle and late Albian) Formations.

The biomicroites and cherts of the Hilo Formation (middle and late Albian TST and HST) reached a high value of 1.93 feet³/ton of hydrocarbons (27.9% out of 6.93 feet³/ton), with a 4.9% TOC average value at the Contador River (RC) in the Villeta area. At Piñal Creek (QP), the hydrocarbon content reached 7.7%, with a 5.8% TOC average value. At Otanche

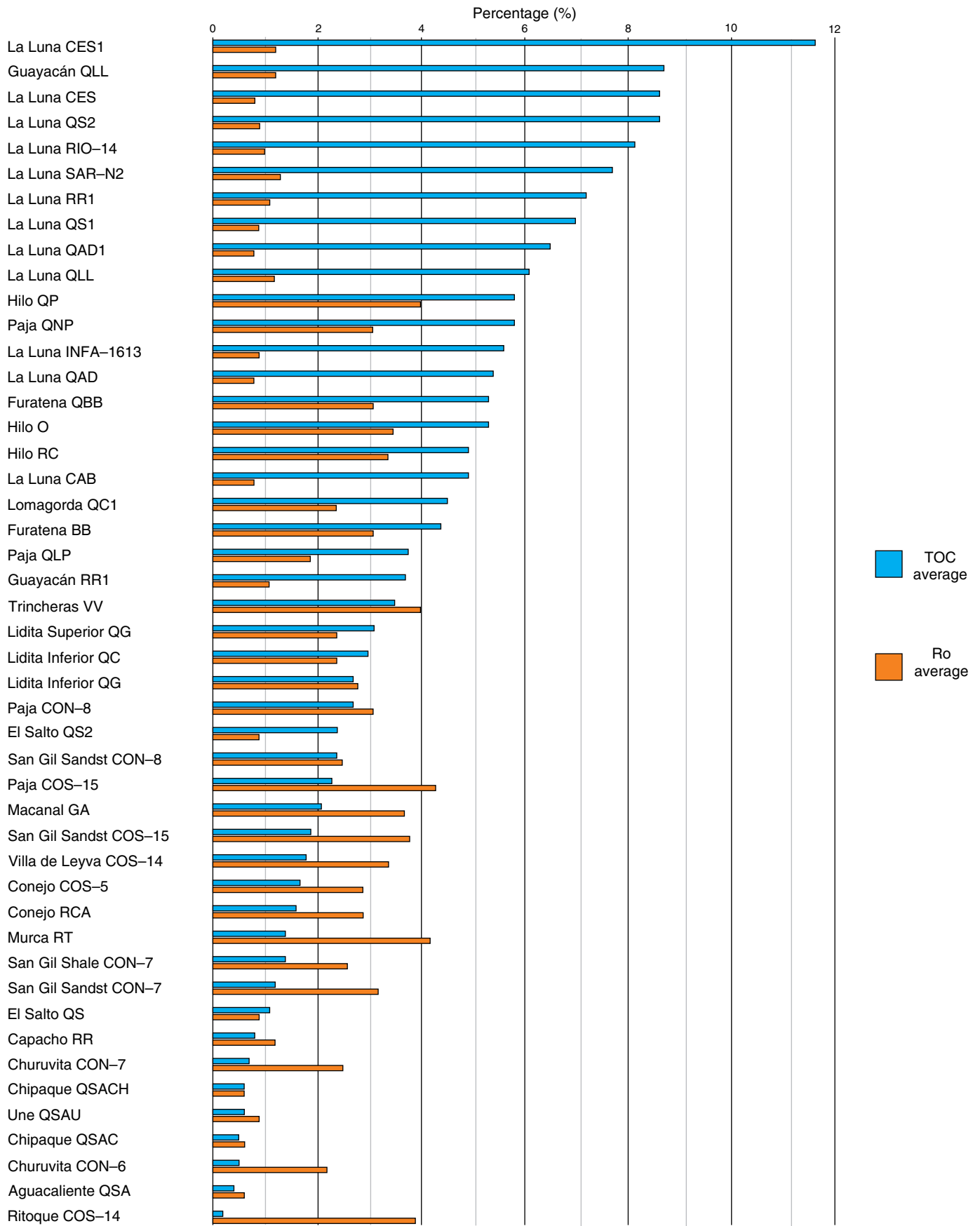




Figure 7. TOC and Ro average values per section. The highest TOC contents (11.6–2.1 %) are from La Luna, Guayacán, Hilo, Paja, Furatena, Lomagorda, Trincheras, Lidita Inferior, Lidita Superior, San Gil Sandstone, and Macanal Formations. The best Ro values (0.8–1.3 %) are from La Luna Formation biomicrites. Number of samples: 1500.

Table 5. Gas chromatography from canisters.

Formation	Sample	Total Gas (feet ³ /ton)	TOC (%)	Ro (%)	Methane % (mol)	Ethane % (mol)	Propane % (mol)	Total HC % (mol)
La Luna	QLL-40	6.56	6.1	PYR 1.2	30.6	15.1	12.1	77.8
La Luna	RR1-25	6.66	7.2	PYR 1.1	19.8	12.6	5.1	47.9
Lidita Inferior	QG-35	10.47	2.7	PYR 2.8	35.1	1.9	0.3	37.3
Lidita Superior	QG-251	12.71	3.1	PYR 2.4	34.2	0	0	34.3
Hilo	RC-16	6.93	4.9	VIT 3.4	27.8	0.1	0	27.9
Guayacán	QLL-00	6.25	8.7	PYR 1.2	13.6	6.6	3	27.2
La Luna	CES1-00	10.55	11.6	PYR 0.8	4.2	3.7	6.4	18.6
Paja	QLP-36	12.61	3.8	PYR 1.9	15.4	1.4	0.2	17.3
Lidita Inferior	QC-13	19.19	3	VIT 2.4	14.6	0.2	0	14.8
La Luna	CES-51	9.34	8.6	PYR 0.8	3.5	2	4.7	13.4
La Luna	CAB-85	12.85	4.9	PYR 0.8	10.6	0	0	10.6
La Luna	QS2-50	15.18	8.6	PYR 0.9	1.8	1.6	2.4	8.5
Hilo	QP-313	13.68	5.8	VIT 4.0	7.7	0	0	7.7
La Luna	QAD-64	8.56	5.4	PYR 0.8	1.6	1	1.9	6.3
La Luna	QAD1-10	13.88	6.5	PYR 0.8	0.9	0.8	1.2	3.7
Conejo	RCA-47	9.66	1.6	PYR 2.9	3.2	0.1	0	3.3
Capacho	RR-00	10.1	0.8	PYR 1.2	0.9	0.2	0.2	1.9
Hilo	O-33	6.02	5.3	VIT 3.5	1.4	0.2	0	1.6
La Luna	QS1-26	8.42	7	PYR 0.9	0.3	0.3	0.4	1.3
Furatena	BB-00	12.8	4.4	VIT 3.1	0.7	0	0	0.7
El Salto	QS2-12	11.6	2.4	PYR 0.9	0.2	0.1	0.2	0.7
Murca (lower section)	RT-29	11.26	1.4	VIT 4.2	0.6	0	0	0.6
Macanal	C-50	8.66	1.4	VIT 2.9	0.5	0	0	0.6
El Salto	QS-03	6.74	1.1	PYR 0.9	0.6	0	0	0.6
Aguacaliente	QSA-93	3.24	0.4	PYR 0.6	0.4	0	0	0.4
Macanal	GA-62	12.42	2.1	VIT 3.7	0.1	0	0.2	0.3
Guayacán	RR1-02	26.55	3.7	PYR 1.1	0.1	0	0	0.2
Macanal	MSP-30	8.67	0.6	VIT 3.0	0.2	0	0	0.2
Trincheras	VV-30	2.2	3.5	VIT 4.0	0.1	0	0	0.2
Une (upper section)	QSAU-19	9.73	0.6	PYR 0.9	0.1	0	0	0.1
Chipaque	QSAC-08	8.38	0.5	PYR 0.6	0.1	0	0	0.1
Fómeque	QED-00	7.22	1.4	VIT 4.2	0.1	0	0	0.1
Fómeque	QLM-00	5.16	1.1	VIT 4.3	0.1	0	0	0.1
Villa de Leyva	RSP-15	12.4	1.3	VIT 3.9	0.004	0	0	0.004
Chipaque	QSACH-22	11.81	0.6	PYR 0.6	0.004	0	0	0.004
Ritoque	RSR-16	9.13	0.6	VIT 3.4	0.004	0	0	0.004
Paja	QNP-06	7.57	5.8	VIT 3.1	0.004	0	0	0.004
Villa de Leyva	QN-00	6.19	0.8	VIT 3.8	0.004	0	0	0.004

Table 6. Gas contents in canister samples (feet³/ton).

Formation	Sample	Lost	Desorbed	Residual	Total Gas	HC (%)	CO ₂ (%)	Total HC	Residual vs. desorbed
La Luna	QLL-40	0.15	1.18	5.24	6.56	77.8	3	5.1	4.5
La Luna	RR1-25	0.08	1.29	5.29	6.66	47.9	7.1	3.19	4.1
Lidita Inferior	QG-35	0.01	0.74	9.72	10.47	37.3	8.5	3.91	13.2
Lidita Superior	QG-251	0.08	6.03	6.6	12.71	34.3	8.9	4.36	1.1
Lidita Inferior	QG-25	0	1.11	6.07	7.17	33.1	9.1	2.37	5.5
Hilo	RC-16	0	1.24	5.69	6.93	27.9	9.8	1.93	4.6
La Luna	QLL-17	0.19	1.11	7.73	9.03	27.6	9.8	2.49	7
Guayacán	QLL-00	0.01	1.27	4.96	6.25	27.2	9.9	1.7	3.9
Lidita Inferior	QG-137	0.01	0.27	4.35	4.63	19.6	10.9	0.91	16.1
La Luna	CES1-00	0.17	1.32	9.06	10.55	18.6	11	1.96	6.9
Lidita Inferior	QG-00	0	0.73	6.9	7.63	18.6	9.9	1.42	9.5
Lidita Superior	QG-261	0.02	0.36	5.7	6.08	18.4	8.4	1.12	15.9
Paja	QLP-36	0.04	0.64	11.92	12.61	17.3	11.2	2.18	18.5
La Luna	RR1-60	0	1.79	13.45	15.24	17.2	11.2	2.62	7.5
La Luna	CES1-21	0.02	1.88	10.54	12.44	15	11.5	1.87	5.6
Lidita Inferior	QC-13	0.05	1.04	18.1	19.19	14.8	11.5	2.84	17.4
La Luna	QLL-09	0.04	1.13	7.33	8.5	13.9	11.7	1.18	6.5
La Luna	CES-51	0.26	1.47	7.61	9.34	13.4	11.7	1.25	5.2
Lidita Inferior	QG-128	0	0.58	4.62	5.21	12.8	10	0.67	7.9
Lidita Inferior	QG-12	0.01	5.03	7.75	12.79	11.7	11.4	1.5	1.5
La Luna	QLL-56	0.63	1.88	8.93	11.44	11.3	11.5	1.29	4.7
La Luna	CES1-10	0.28	2.64	12.2	15.11	10.6	12.1	1.6	4.6
La Luna	CAB-85	0.07	1.35	11.44	12.85	10.6	12.1	1.36	8.5
La Luna	QS2-50	0	1.97	13.21	15.18	8.5	12	1.29	6.7
Lidita Inferior	QG-55	0	0.39	3.06	3.45	8.2	12.4	0.28	7.8
Paja	QLP-55	0.03	0.98	8.29	9.31	8	12.4	0.74	8.4
La Luna	CAB-32	0.05	1.3	16.77	18.13	7.8	12.5	1.41	12.9
Hilo	QP-313	0.02	3.83	9.84	13.68	7.7	12.5	1.05	2.6
La Luna	CES-24	0.61	2.22	12.47	15.3	7.6	12.5	1.16	5.6
La Luna	CES-15	0.16	1.77	8.67	10.6	6.9	12.6	0.73	4.9
Paja	QLP-44	0.01	0.86	9.81	10.68	6.8	12.6	0.73	11.4
La Luna	RR1-35	0.16	2.17	12	14.32	6.4	12.7	0.92	5.5
La Luna	QAD-64	0.15	1.34	7.08	8.56	6.3	12.9	0.54	5.3
La Luna	CAB-15	0.13	1.27	6.67	8.07	5.8	12.4	0.47	5.3
La Luna	QS2-38	0.04	1.9	12.33	14.28	4.4	12.9	0.63	6.5
La Luna	QAD-53	0.12	1.13	10.31	11.56	4.4	13.1	0.51	9.2
La Luna	QS2-25	0.02	1.29	16.14	17.45	4.4	13.1	0.77	12.6
La Luna	QAD1-10	0.05	1.12	12.71	13.88	3.7	13.1	0.51	11.4
Conejo	RCA-47	0	0.03	9.63	9.66	3.3	12.7	0.32	367.3
La Luna	QAD1-60	0.28	1.71	10.86	12.85	3	13.2	0.39	6.4
Conejo	RCA-59	0.05	0.21	3.91	4.17	2.1	13.3	0.09	19
Capacho	RR-00	0.26	1.32	8.52	10.1	1.9	11.7	0.19	6.5
Hilo	O-33	0.07	0.81	5.14	6.02	1.6	13.3	0.1	6.4

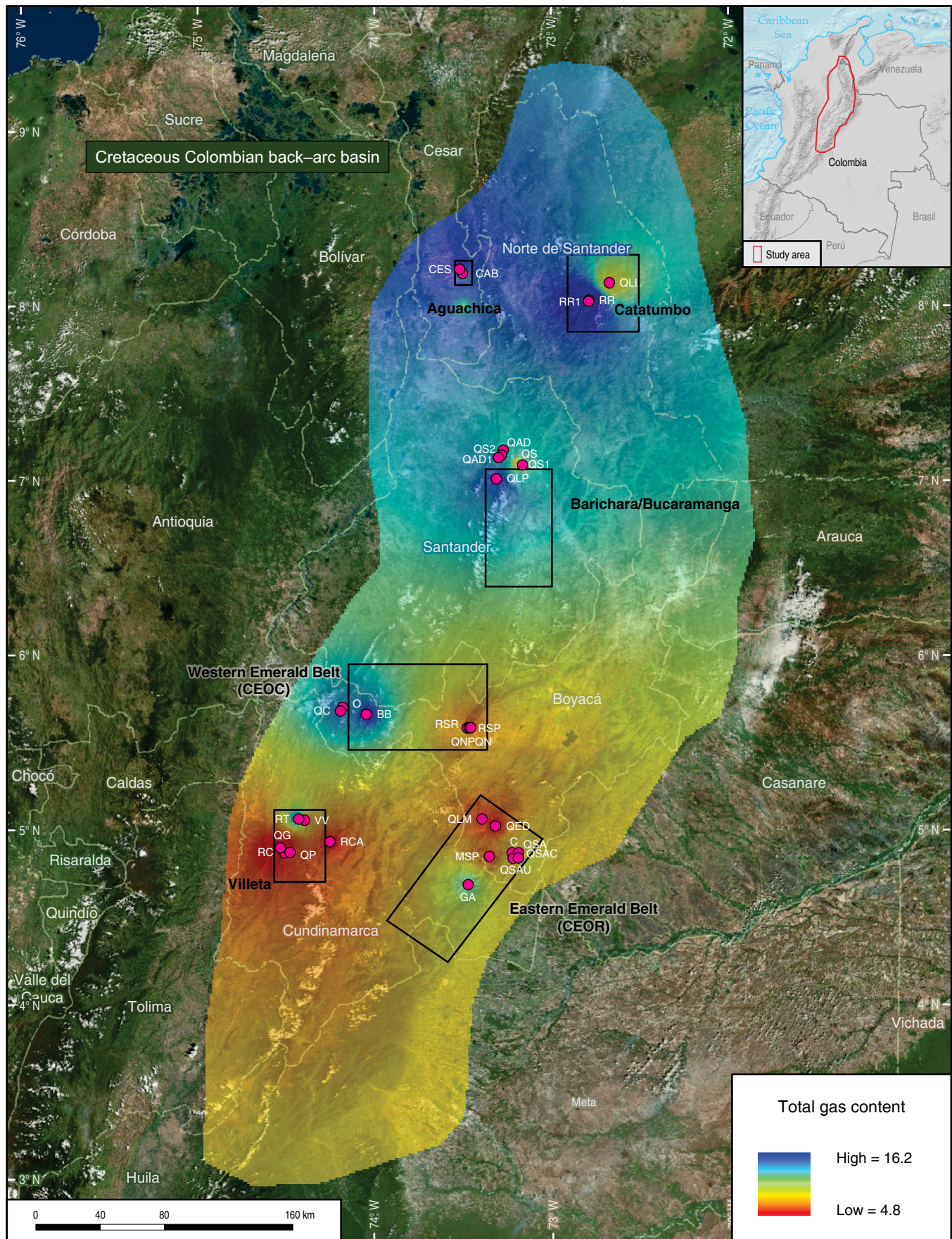


Figure 8. Total gas content average per section (feet³/ton), including hydrocarbons, CO₂, nitrogen, and oxygen. Number of samples: 200.

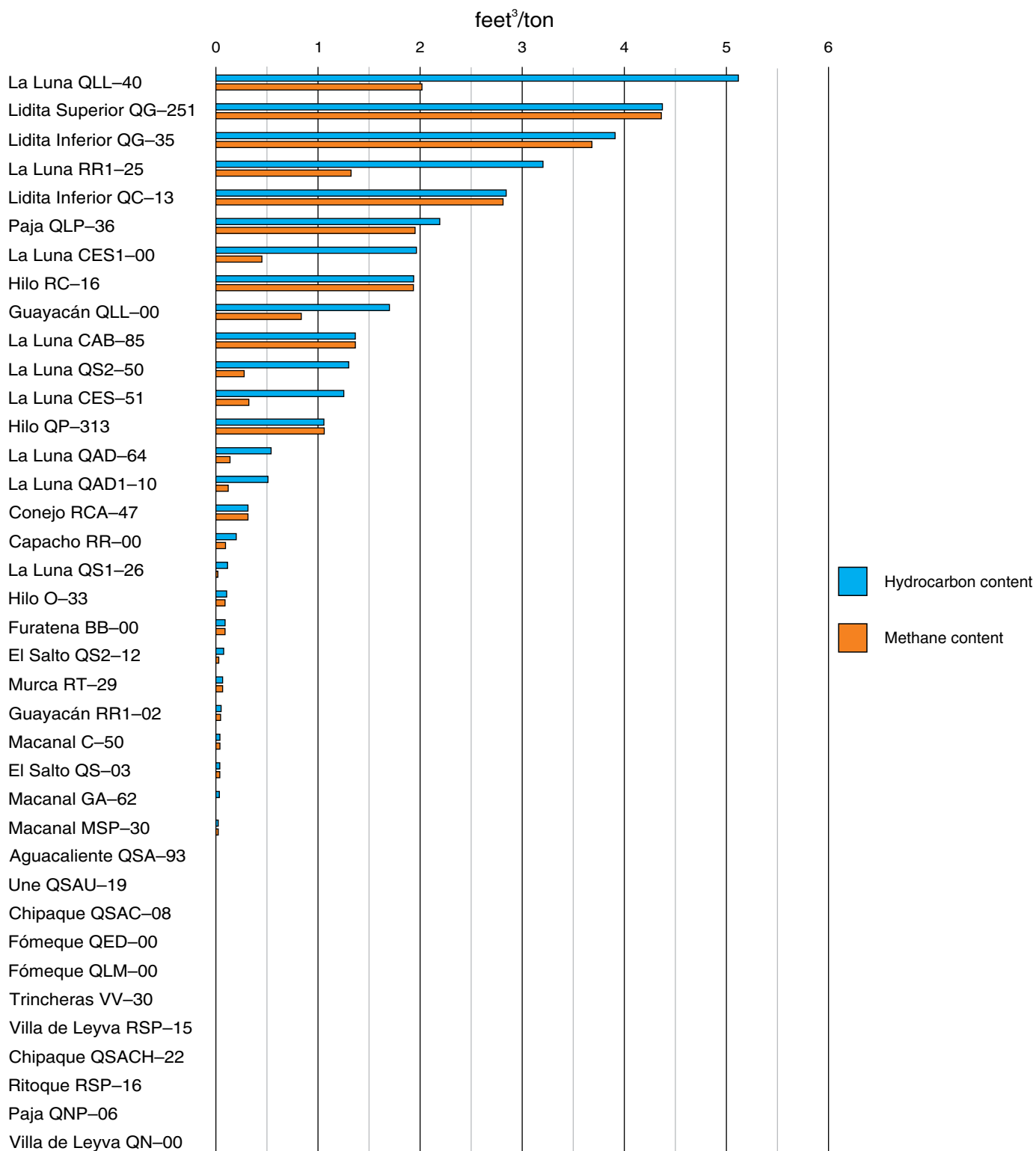


Figure 9. Samples with the highest hydrocarbon volume (feet³/ton), along with their methane content. The best samples are from La Luna, Lidita Superior, Lidita Inferior, Paja, Hilo, and Guayacán Formations.

(O), the hydrocarbon content reached 1.6%, with a 5.3% TOC average. The highest TOC value of the Hilo Formation (12.1%) comes from sample O-10 at the Otanche section. The Capacho Formation shales from the same time span in the Cúcuta area

present lower values: 1.9% for the highest hydrocarbon content and only 0.8% TOC average.

The best sample of the Paja Formation (Barremian and Aptian TST and HST) from the type section at the Paja Creek

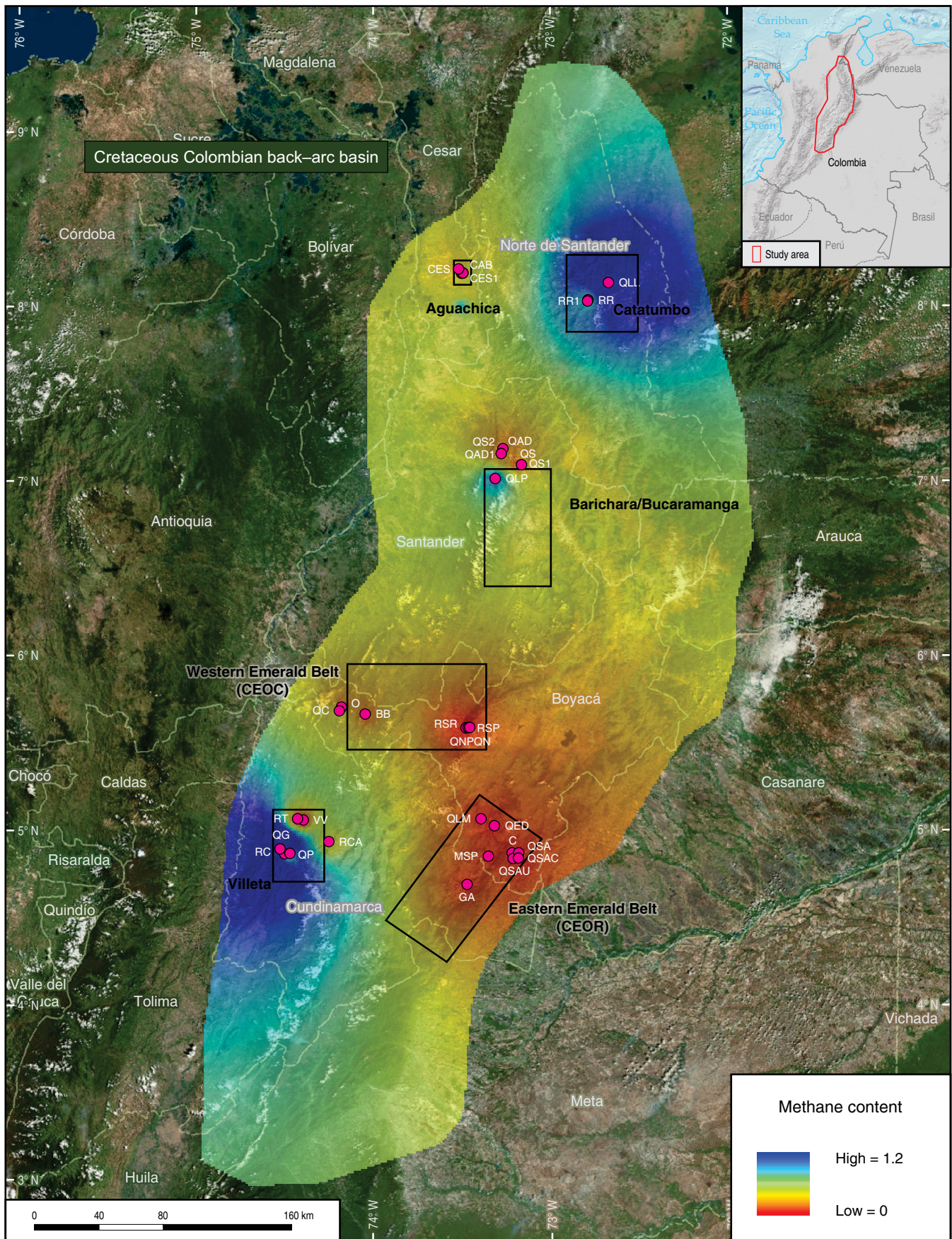


Figure 10. Methane average volumes per section (feet³/ton). Total number of samples: 200.

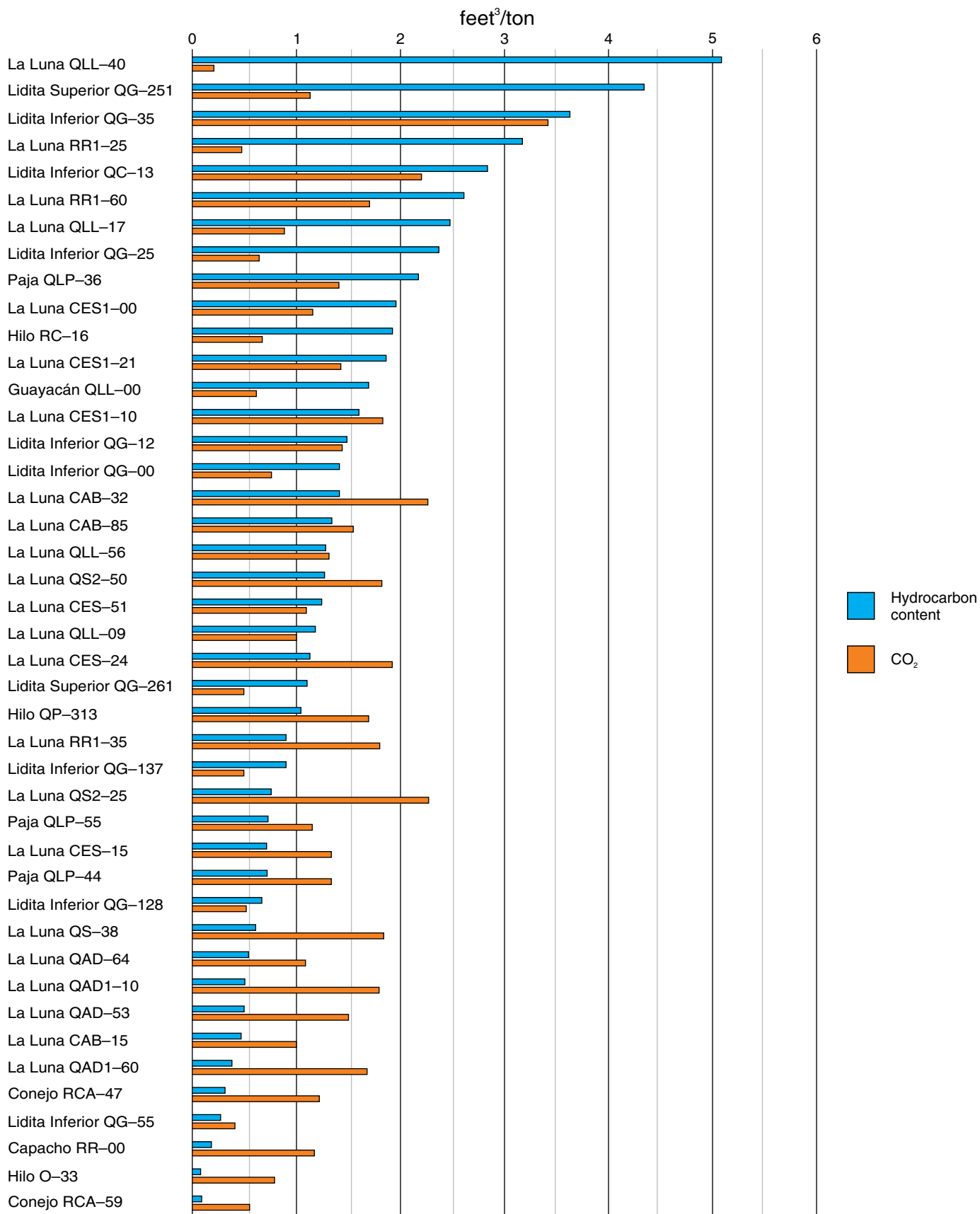


Figure 11. Samples with the highest hydrocarbon volume (feet³/ton), along with their CO₂ content. The best hydrocarbon contents are from La Luna, Lidita Superior, Lidita Inferior, Paja, Hilo, and Guayacán Formations.

(QLP-36) released 12.61 feet³/ton of gas, of which 17.3% (2.18 feet³/ton) are hydrocarbons; the average TOC of the section is 3.8%, but the highest value of the unit is 9.7% TOC from sample QLP-08. Thermal maturity from pyrolysis is 1.9%, so the unit is in the gas window.

All the other units had very low percentages of hydrocarbons in the gas contents in the canister measurements, ranging from 0.004 to 0.7% in the Furatena, Murca, Trincheras, Paja, El Salto, Guayacán, Macanal, Fómeque, Une, Chipaque, Aguacaliente, Ritoque, and Villa de Leyva Formations (Figure 9; Table 6). These units are composed mainly of shale, with minor interbedding of marlstone and biomicroite. In most samples, the gas measured was a mixture of oxygen and nitrogen introduced during air exposure close to the surface.

In samples with the highest contents of hydrocarbons from La Luna Formation, the volumes of residual gas released after fracturing the canister samples were always higher (4.1 to 12.9 times, with an average of 6.8 times) than the volumes of gas desorbed before fracturing and milling (Table 6). This means that these rocks still have hydrocarbons stored in micropores and microfossil cavities that can be released by fracturing, simulating the induced fracking process at depth. The sample with the highest volume of hydrocarbons (5.10 feet³/ton) was QLL-40 from La Luna Formation in the Cúcuta area, which released 4.5 times more residual than desorbed gas. According to ICP-MS elemental analyses and petrography, QLL-40 is a partially silicified biomicroite composed of foraminifera with 65% calcite, 30% quartz, and less than 1% Al₂O₃. Sample RR1-60 from La Luna Formation in the Cúcuta area, which is also a partially silicified biomicroite with 47% calcite, 47% quartz, and less than 2% Al₂O₃, contained a hydrocarbon volume of 2.62 feet³/ton and a ratio of 7.5 residual versus desorbed gas.

Sample CES1-00 from the Aguachica area, which is a pure biomicroite with 96% calcite and less than 1% Al₂O₃, released a hydrocarbon volume of 1.96 feet³/ton and had a ratio of 6.9 times residual versus desorbed gas. Samples CAB-85 from Aguachica and QS2-50 from Barichara are partially silicified biomicroites with 75% calcite, 13–15% quartz, 4–5% clay minerals, 2–3% fluorapatite phosphates, 1% ankerite, and 1–2% pyrite. Sample CAB-85 released gas hydrocarbons in a concentration of 1.36 feet³/ton and had a ratio of residual versus desorbed gas of 8.5. Sample QS2-50 released 1.29 feet³/ton and had a ratio of residual versus desorbed gas of 6.7. This means that regardless of the partial replacement of calcite by quartz, La Luna Formation biomicroites and diagenetic cherts (with clay mineral contents below 5%) have similar properties and contain important volumes of hydrocarbons of marine origin.

The best samples of the Lidita Inferior and Lidita Superior of the Oliní Group present a less uniform ratio of residual versus desorbed gas. At Guate Creek (QG), the residual to desorbed gas ratio varies from 1.1 to 16.1 times, and at Cobre Creek (QC), it is 17.4 times. The volumes of gas hydrocarbons

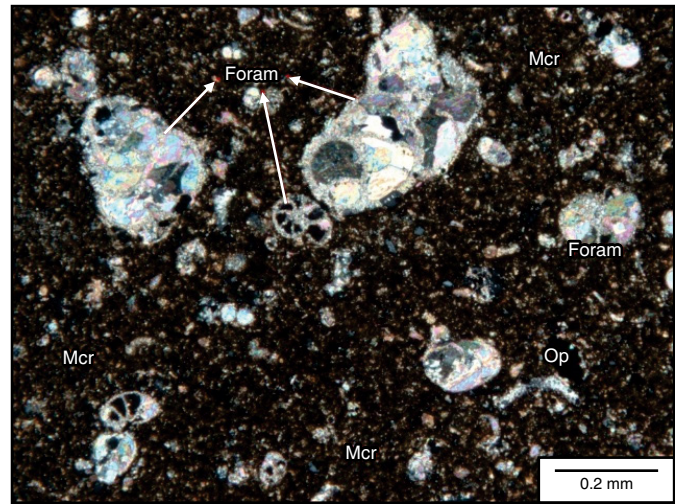


Figure 12. Thin section photograph of a silicified biomicroite (sample QG-251) from the Lidita Superior at Guate Creek west of the Bituima Fault. Large foraminifera have a length of 100 to 300 μm . The matrix is composed of organic matter and partially silicified calcareous mud (silt-sized fragments of foraminifera and calcareous algae). The sample contains 15% terrigenous mud (clay minerals and silt-sized quartz particles), 50% diagenetic quartz, and 35% calcite.

range from 0.28 to 4.36 feet³/ton, which are similar to those of La Luna Formation, but there are fewer samples with gas in this unit than in La Luna. The lithology of the Lidita Units at Guate Creek (Figure 12) is slightly different from that of La Luna, with a higher clay mineral content between 10 and 30%, a calcite content of 25 to 45%, and a quartz content (in the form of diagenetic chert and silt-sized particles) of 20–75%. The section QC contains an average of 59% quartz (diagenetic chert and silt-sized particles), 39% clay minerals, and less than 1% calcite.

The best samples of the Hilo Formation from the Contador River (RC) and Piñal Creek (QP) released gas hydrocarbons in similar concentrations to La Luna, but there are very few of them compared with the number from La Luna. The RC samples are impure biomicroites and marlstones with 20–30% clay minerals, 25–55% calcite, and 32–58% quartz (diagenetic chert and silt-sized particles). The sample RC-16 released 1.93 feet³/ton and had a ratio of 4.6 residual versus desorbed gas. The QP samples are impure biomicroites and marlstones with 10–40% clay minerals, 10–70% calcite, and 21–77% quartz (diagenetic chert and silt-sized particles). Sample QP-313 released 1.05 feet³/ton and had a ratio of 2.6 residual versus desorbed gas.

Other units that released hydrocarbons include the Paja, Capacho, and Conejo Formations. Sample QLP-55 from the type section of the Paja Formation is a marlstone with 50% calcite, 25% clay minerals, 20% silt-sized quartz particles, and 5% pyrite; the sample released gas hydrocarbons with a concentration

of 0.74 feet³/ton. The Paja Formation is composed of shale with minor marlstone and biomicrite; the samples of the QLP section contain 10–75 % clay minerals, 2–60% calcite, 5–30 % quartz, and 3–10% pyrite. Sample QLP–36 released gas hydrocarbons with a concentration of 2.18 feet³/ton, which is comparable with good samples from La Luna Formation.

The samples RCA–47 and RR–00 from the Conejo and Capacho Formations released smaller amounts of hydrocarbons (0.32 and 0.19 feet³/ton) than samples from La Luna Formation. The Conejo Formation from section RCA is composed of shale with minor marlstone and chert; it contains 10–60 % clay minerals, 20–70 % quartz (in silt particles and diagenetic chert), 2–32 % calcite, and 2–5 % pyrite. The Capacho Formation is composed of shales with less than 2% calcite, 40–50 % clay minerals, and 50–60 % silt-sized quartz particles.

The samples of the units with higher clay contents tend to have an erratic relationship of residual versus desorbed gas. This was especially notable in the Conejo Formation (19.0 to 367.3 times), which is very different from the more uniform relationship (4.1 to 12.9 times) of the biomicrites and cherts from La Luna Formation. It seems that the shales exposed near the surface (3 m depth) are more fractured and weathered than the biomicrites, so the relationship of residual versus desorbed gas (mostly air in the Conejo Formation) is less uniform.

The residual gas contents (Table 6) of samples from field exposures of the Paja, Capacho, Guayacán, La Luna, Lidita Inferior, and Lidita Superior Formations (3.06 to 18.10 feet³/ton) are comparable with the residual gas contents (3.13 to 24.33 feet³/ton) of samples from a well (534 to 564 m depth) in a Paleozoic shale in Indiana by Mastalerz et al. (2016). However, the ratios of desorbed to residual gas content are not comparable because the amount of desorbed gas was always higher than the amount of residual gas (a ratio of 1.1 to 7.4) in the well samples from Indiana (Mastalerz et al., 2016), but in our samples, it was the opposite: the amount of residual gas was always higher than the amount of desorbed gas (a ratio of 1.1 to 18.5). We conclude that most of the total desorbed gas originally present in our samples was lost during uplift decompression and fracturing and during weathering close to the surface (3 m depth). If the relationship of residual gas in our best samples (in terms of hydrocarbon and residual gas content) from La Luna, Paja, and Lidita Inferior Formations (CES1–00, QLP–36, and QC–13) is extrapolated to the total gas they should contain at depth, using the average ratio of total to residual gas (approximately 5) of Mastalerz et al. (2016), total gas values between 45.5 and 90.5 feet³/ton could be reached. A clear relationship of increasing gas content (18.8 to 67.8 feet³/ton) with increasing organic matter content (1.22 to 15.61% TOC) was documented by Mastalerz et al. (2016), who indicated that the gas was contained mainly within the micropores of the organic matter. We also found that the samples with the highest TOC generally contained the highest amounts of gas hydrocarbons.

Table 7. Porosity and permeability.

Formation	Section	Porosity (%)	Permeability (μ D)	Hydrocarbons (% molar)
Guayacán	QLL	0.28	0.01	27.15
Lidita Inferior	QG	0.43	0.08	15.03
Lidita Superior	QG	0.89	2.12	16.94
La Luna	CES	0.96	0.68	3.51
Ritoque	RSR	0.97	0.17	0
La Luna	RR1	1.18	0.09	18.24
La Luna	CAB	1.31	11.01	2
Conejo	RCA	1.34	14.92	2.28
La Luna	CES1	1.47	0.52	11.93
Furatena (lower section)	BB	1.55	0.21	0.46
Villa de Leyva	RSP	1.8	0.56	0
La Luna	QAD	1.93	6.14	4.05
Macanal	C	2.01	26.27	0.11
Fómeque	QED	2.06	13.15	0.02
Murca (lower section)	RT	2.44	24	0.23
La Luna	QLL	2.56	3.04	26.21
La Luna	QS1	2.67	0.2	1.02
La Luna	QAD1	2.67	0.24	1.89
La Luna	QS2	3	4.85	5.77
Villa de Leyva	QN	3.03	247.33	0
Hilo	QP	3.05	62.33	1.12
Macanal	MSP	3.23	17.88	0.07
Macanal	GA	3.27	23.56	0.08
Fómeque	QLM	3.44	118.63	0.02
Une (upper section)	QSAU	3.65	0	0.03
Lidita Inferior	QC	3.83	7.72	3.38
Trincheras	VV	4.09	57.54	0.07
Guayacán	RR1	4.32	2235.26	0.1
Aguacaliente	QSA	4.59	64.58	0.05
Capacho	RR	4.66	16 560.92	1.09
El Salto	QS	5.22	26.63	0.41
El Salto	QS2	5.27	4094.03	0.51
Chipaque	QSAC	5.38	36 853.87	0.01
Chipaque	QSACH	5.65	45.28	0
Hilo	RC	7.43	0.76	7.47
Paja	QNP	10.01	61.09	0
Hilo	O	20.8	255.87	0.38

4.3. Porosity and Permeability

The limestones and cherts of the Guayacán, La Luna, Lidita Inferior, and Lidita Superior Formations, which released the

highest average percentages of gaseous hydrocarbons (11.93–27.15 %), have porosity values below 3% and absolute permeability below 3 microdarcys (Table 7). In contrast, the shale units have higher and nonreliable values, which reached 20.8% porosity in shales of the Hilo Formation and 36 854 microdarcys (36.85 millidarcys) in shales of the Chipaque Formation. These abnormal porosity and permeability values for the shales should correspond to free space produced during fracturing and weathering and to noneffective porosity related to water bounded to clay minerals. On the other hand, the low porosity and very low permeability values of the limestones, which have the highest contents of gas, do not necessarily account for all the nonconnected pores and fossil cavities, which can preserve hydrocarbons.

La Luna Formation biomicrites have uniform porosity values between 1 and 3%, with permeability values between 0.1 and 11 microdarcys. The biomicrites and cherts of the Lidita Inferior and Lidita Superior Formations also have uniform values of porosity (below 4%) and permeability (below 8 microdarcys). There are also shale units (Murca, Macanal, Fómeque, and Conejo Formations) with comparable values of porosity (below 4%) and permeability (13 to 26 microdarcys), but those units contained very little or no hydrocarbons.

The values presented here for La Luna Formation are comparable with those obtained by Cerón et al. (2013) and Walls et al. (2014) for the MMV and Catatumbo areas; the authors also showed that La Luna average values are comparable to those of the Eagle Ford reservoir from Texas. They used a high resolution microCT scanner and SEM imaging to obtain average porosity values of 4.8–6.3 % and average horizontal permeability values of 733 to 920 nanodarcys (0.73 to 0.92 microdarcys). They also reported solid organic material of 7.7–8.1 % and porosity values of 20–29 % within that organic material.

The very low permeability values that we obtained from the limestones of the Guayacán, La Luna, Lidita Inferior, and Lidita Superior Formations are very good because they mean that the units still retain hydrocarbons in organic matter, nonconnected pores, and fossil cavities, which could be released by fracking.

4.4. Pyrolysis and Organic Geochemistry

The pyrolysis results reveal that La Luna Formation limestones have the best indicators in terms of hydrocarbon content, type II organic matter, and thermal maturity (Figures 13, 14; Table 8). The best sections (QAD1, QAD, CES, INFAN-1613, CES1, CAB, QS1, and QS2) are in the NW sector of the basin, in the areas of Aguachica and Barichara/Bucaramanga, in the MMV and W foothills of the Eastern Cordillera, followed by the Cúcuta sections in the Catatumbo area (RIO-14, SAR-N2, RR1, and QLL), in the NE sector of the basin. Older units, with a higher shale and marlstone content, including the Paja, Simití, El Salto, Capacho, and Guayacán, are also in the oil and gas

generation windows and have significant amounts of type III and type II kerogens.

Table 8 compiles the parameters of pyrolysis of units with higher hydrocarbon contents, which in La Luna Formation from the MMV and W flank of the Eastern Cordillera reach averages between 9.48 and 23.29 mg HC/g at the S2 peak. The best S2 average values of sections from La Luna Formation are above the average values reported from the Aguablanca section (4.54 mg HC/g) W of Bucaramanga (Casadiego & Rios, 2016) and 13.21 mg HC/g from a well in the Maracaibo area of Venezuela (Liborius & Slatt, 2014). The last one is comparable with the average (13.02 mg HC/g) from La Sorda Creek (QS1) W of Bucaramanga. The S2 averages from the Catatumbo area are lower (2.14 to 7.93 mg HC/g) because the sections have a higher thermal maturity (451 to 473 °C Tmax) and have released more hydrocarbons than the ones from the MMV and W foothills of the Eastern Cordillera (440 to 446 °C Tmax). Aguilera et al. (2010) reported S2 values from the MMV between 1 and 20 mg HC/g, with most data points between 5 and 15 mg HC/g, with Tmax values between 430 and 450 °C. Aguilera et al. (2010) also reported S2 values from Catatumbo below 10 mg HC/g.

Values lower than 0.2 mg HC/g at S1 and S2 are present in overmature units that have lost nearly all hydrocarbons; in those samples, the values of Tmax are unreliable and do not permit deducing the thermal maturity of the units (e.g., Nuñez-Betelu & Baceta, 1994). For example, the Paja Formation from well COS-15 presents very low average values of S1 (0.16 mg HC/g) and S2 (0.13 mg HC/g) so that the values of Tmax are erroneously low, approximately 322 °C, which would indicate that the unit has not entered the generation window. However, the correct value of vitrinite reflectance (4.3% Ro) indicates that the unit is overmature. The same goes for the other units of the Agencia Nacional de Hidrocarburos (ANH) wells from the Eastern Cordillera, which in general are overmature and have already released most of their hydrocarbons.

The hydrogen index (HI) averages are generally higher in the biomicrite limestones, which have a greater marine contribution of organic matter, than in the shales, which have a more terrestrial contribution along with the clay minerals (Figures 15–17; Table 8). The average values of La Luna Formation biomicrites in the MMV on the NW side of the basin ranged from 81 to 292, suggesting mixtures of types II–III of marine and continental origin. The average HI values of La Luna from the Catatumbo area in the NE side of the basin ranged from 24 to 112, suggesting a higher contribution of organic matter type III of continental origin; the Catatumbo samples also have higher production index (PI) values and higher thermal maturity (Ro 1–1.3 %) than those of the MMV (Ro 0.8–0.9 %). Aguilera et al. (2010) reported that most samples from the Catatumbo area had poor generation potential, with HI values below 200 and S2 values below 5, indicating

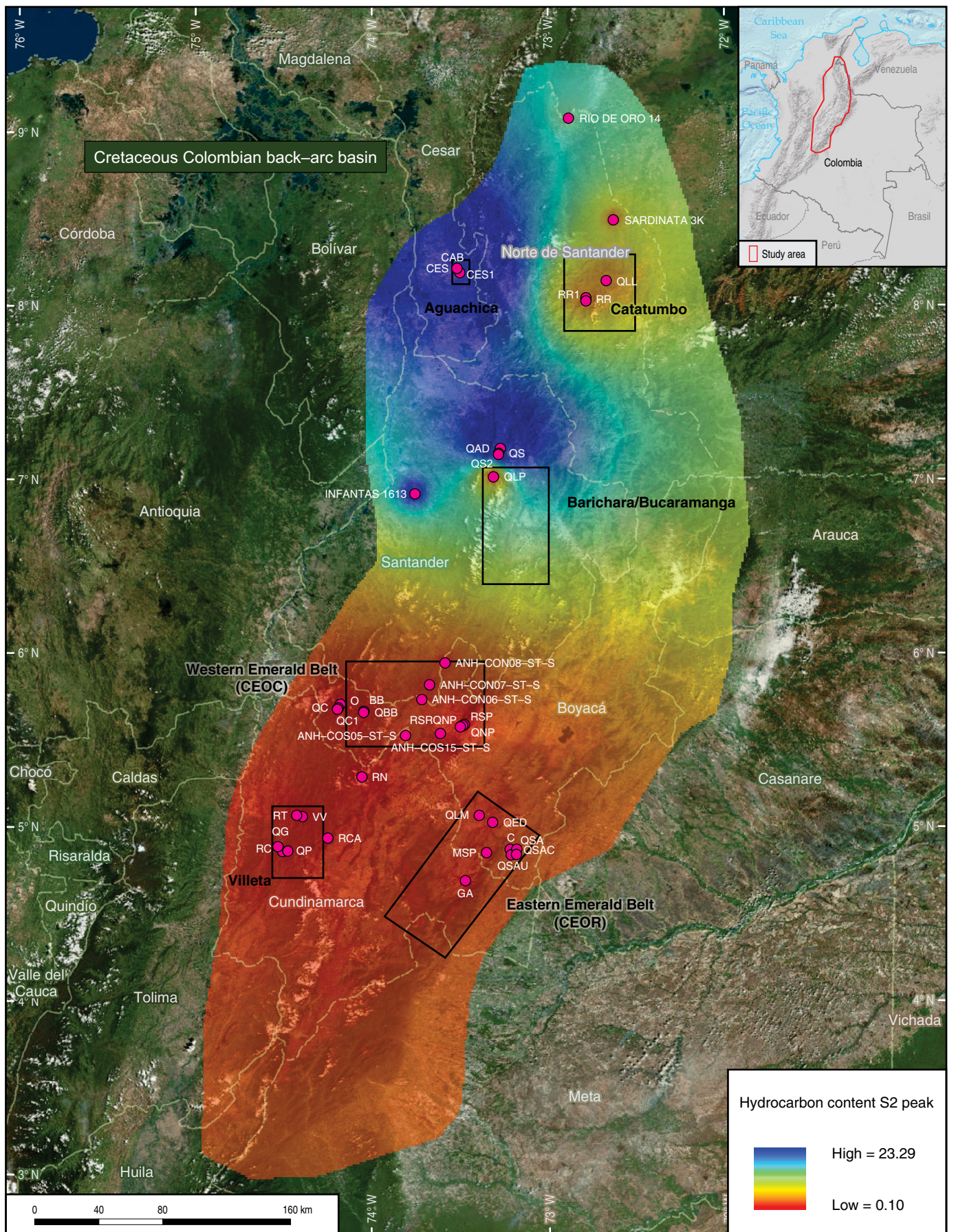




Figure 13. Average hydrocarbon contents (mg HC/g) per section at the S2 peak. The best values are located in the NW sector of the basin. Total number of samples: 500.

Table 8. Pyrolysis.

Formation	Section	TOC (%)	Ro (%) VIT-PYR	S1 (mg HC/g) ^a	S2 (mg HC/g) ^b	Tmax (°C) ^c	HI	PI
La Luna	QAD1	8.3	PYR 0.8	4.69	23.29	444	281	0.17
La Luna	QAD	7.2	PYR 0.8	4.46	19.45	443	292	0.18
La Luna	CES	10.5	PYR 0.8	2.06	19.06	440	182	0.1
La Luna	INFA-1613	7.7	PYR 0.9	4.04	18.81	446	250	0.18
La Luna	CES1	11.9	PYR 0.8	1.34	17.67	441	149	0.07
La Luna	CAB	6.8	PYR 0.8	1.47	16.15	442	252	0.08
La Luna	QS1	8.6	PYR 0.9	2.61	13.02	445	151	0.17
La Luna	QS2	10.9	PYR 0.9	1.17	9.48	446	81	0.13
La Luna	RIO-14	8.1	PYR 1.0	2.53	7.93	451	112	0.24
La Luna	SAR-N2	9.6	PYR 1.3	1.3	2.68	468	28	0.34
La Luna	RR1	9.8	PYR 1.1	0.73	2.37	457	24	0.26
La Luna	QLL	8.6	PYR 1.2	0.64	2.14	473	25	0.24
Chipaque	QSACH	0.8	PYR 0.6	0.05	1.23	431	123	0.08
Paja	QLP	6	PYR 1.9	0.19	0.85	502	15	0.2
Aguacaliente	QSA	0.5	PYR 0.6	0.04	0.85	430	152	0.07
Lidita Superior	QG	3.6	PYR 2.4	0.16	0.61	530	17	0.2
Lidita Inferior	QG	3.7	PYR 2.8	0.11	0.54	551	15	0.19
Chipaque	QSAC	0.6	PYR 0.6	0.04	0.54	431	90	0.08
Capacho	RR	1.2	PYR 1.2	0.25	0.44	464	38	0.36
Conejo	RCA	2.6	PYR 2.9	0.09	0.27	560	11	0.26
Paja	COS-15	3.3	VIT 4.3	0.16	0.13	322	4	0.52
Paja	CON-8	5.1	VIT 3.1	0.09	0.11	345	2	0.46
Villa de Leyva	COS-14	1.9	VIT 3.4	0.08	0.11	336	6	0.42
Conejo	COS-5	4.3	VIT 2.9	0.08	0.11	409	5	0.42
San Gil Shale	CON-7	1.7	VIT 2.6	0.07	0.1	373	6	0.4

^a Volume of hydrocarbons that formed during thermal pyrolysis at ca. 300 °C.

^b Volume of hydrocarbons that formed during thermal pyrolysis at Tmax.

^c Temperature of maximum hydrocarbon generation.

that it could also reflect the depletion effect caused by the high thermal maturity of the Cretaceous rocks.

The hydrogen index values should be treated with caution when interpreting the type of organic matter because the samples that released the highest amounts of hydrocarbons are silicified biomacrites composed of foraminifera, with less than 5% terrigenous particles. For instance, sample QAD1-20 from the W foothills of the Eastern Cordillera, which had a TOC of 8.2%, released 4.13 mg HC/g at S1 and 18.22 mg HC/g at an S2 peak Tmax of 444 °C and had an HI of 221, which would indicate a mixture of terrestrial and continental type II-III organic matter. However, the sample has less than 5% clay min-

erals, 50% calcite, 5% dolomite, and 40% diagenetic quartz, according to the petrography, XRD, and ICP-MS analyses; the framework of the rock was composed of planktonic foraminifera and fish bones. It is difficult to believe that a rock that has so little terrigenous particles could have important amounts of type III organic matter. As indicated by Nuñez-Betelu & Baceta (1994), it is possible to chemically degrade organic matter type II into type II-III due to variations in the mineral matrix and organic enrichment. We believe that the main reason for the low HI values is the relatively high thermal maturity of the samples, but it is also possible that the exchange of calcite by quartz and fluorapatite during diagenesis could have affected the carbon

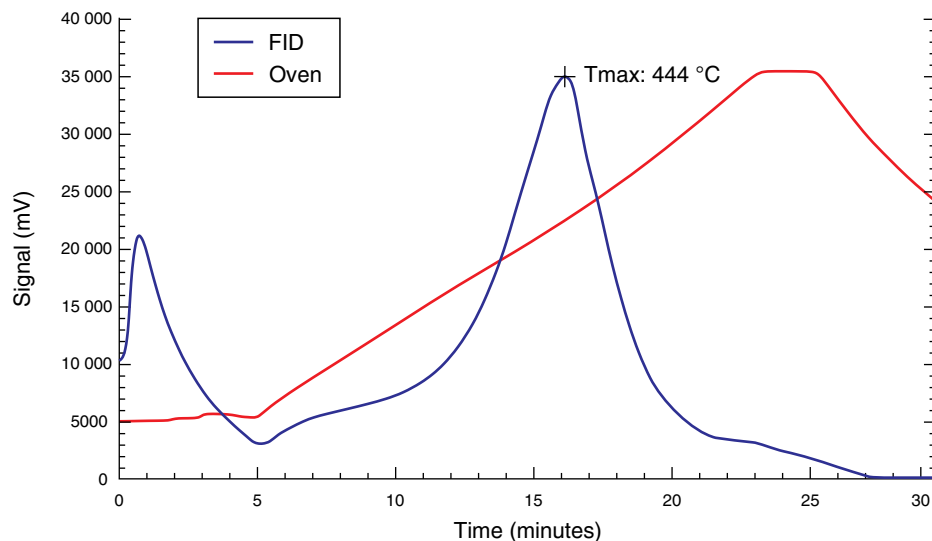


Figure 14. Pyrogram of sample QAD1–20 from La Luna Formation in the Aguadulce Creek section of the Barichara area.

and hydrogen relationships of La Luna Formation biomicrites and diagenetic cherts. The highest hydrogen index value from the Aguadulce Creek section is 450, from sample QAD1–46, which released 37.65 mg HC/g at an S2 peak Tmax of 440 °C, indicating fully marine–origin type II organic matter.

An interesting example of a very low hydrogen index of 14, erroneously indicating a terrestrial type III organic matter, comes from sample QLL–40 from the Catatumbo area. It had a TOC of 7.4%, released 0.51 mg HC/g at S1 and 1.04 mg HC/g at an S2 Tmax of 471 °C. According to ICP–MS elemental analyses and petrography, QLL–40 is a partially silicified biomicrite of foraminifera with 65% calcite, 30% diagenetic quartz, and less than 1% Al_2O_3 . Again, it is difficult to believe that a rock made of planktonic foraminifera and with so little clay mineral content could have important amounts of type III continental organic matter. As indicated before, sample QLL–40 released the highest amounts of gaseous hydrocarbons (canister measurements) in the entire study. This is not because of the type of organic matter but because La Luna Formation in the Catatumbo area is more mature (1.3% Ro) than that in the Magdalena Valley. We believe that in addition to the relatively high thermal maturity of the samples, the diagenetic changes involving quartz and phosphate replacement of calcite affected the carbon and hydrogen relationships of the samples. In La Leche Creek section, the highest HI is 60, from sample QLL–10, which is again a partially silicified biomicrite of foraminifera with 50% calcite, 40% diagenetic quartz, 3% pyrite and dolomite, and 5% clay minerals, which could not have had enough terrestrial influx to predominantly incorporate type III organic matter of continental origin.

Another indication of the type of organic matter from the Catatumbo area is expressed by the ratio of tricyclic terpanes

(Figure 18), indicating the relative presence of carbonates and clay minerals or marine versus terrestrial organic matter. In oils with organic matter of marine origin, C_{23} is the dominant terpane, and C_{25} is more abundant than C_{26} (e.g., Peters & Moldowan, 1993). However, it is interesting to consider the known mineralogy of the samples, according to the available petrography, ICP–MS elemental analyses, and XRD. Sample RR1–02 from the Guayacán Formation (on the right side of the Figure 18) is a shale with 60% clay minerals and 40% silt-sized quartz particles. Samples RR–6, 18, and 20 from the Capacho Formation (at the center of the Figure 18) are also shales with 50–60 % clay minerals and 40–50 % silt-sized quartz particles. Samples RR1–20 to RR1–40 from La Luna Formation are partially silicified biomicrites of foraminifera with 40–98 % calcite, 2–50 % diagenetic quartz, and 2–8 % clay minerals; all of them fall on the left (carbonate) side of the Figure 18, except for RR1–28. Samples QLL–04 to QLL–40 from La Luna Formation are also partially silicified biomicrites composed of foraminifera with 45–65 % calcite, 30–50 % diagenetic quartz, and 2–12 % clay minerals; all of them fall on the left (carbonate) side of the Figure 18, except for QLL–40. This means that except for a few samples, the type of organic matter is better expressed by the ratio of tricyclic terpanes than by using the hydrogen index previously discussed.

The tricyclic terpane ratio of the samples from the MMV and W foothills of the Eastern Cordillera (Figure 19) indicates a predominance of marine organic matter. Most samples fall on the left side of the Figure 19, except for some samples of the Paja (QLP) and La Luna (CAB, CES1) Formations. According to the available petrography, ICP–MS elemental analyses, and XRD, the Paja Formation at its type section is composed of marlstones and shales with minor biomicrite interbedding,

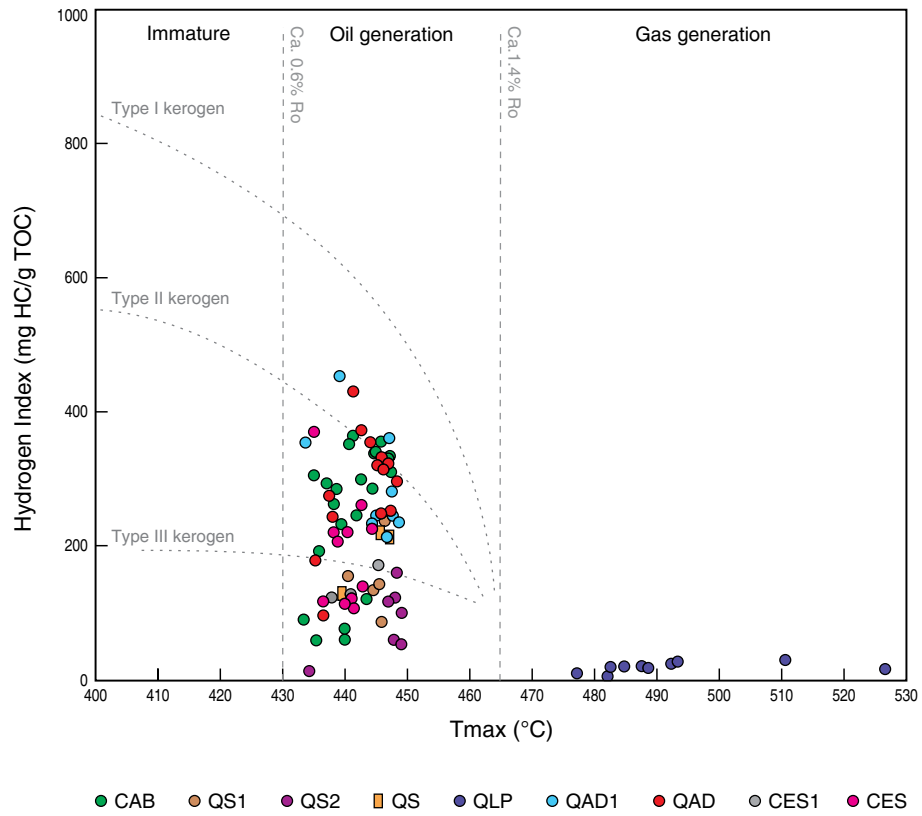


Figure 15. HI vs. Tmax of the Paja (QLP), Simití (QS), El Salto (QS2), and La Luna (QAD, QAD1, CES, CES1, CAB, QS1, QS2) Formations from the MMV and W foothills of the Eastern Cordillera.

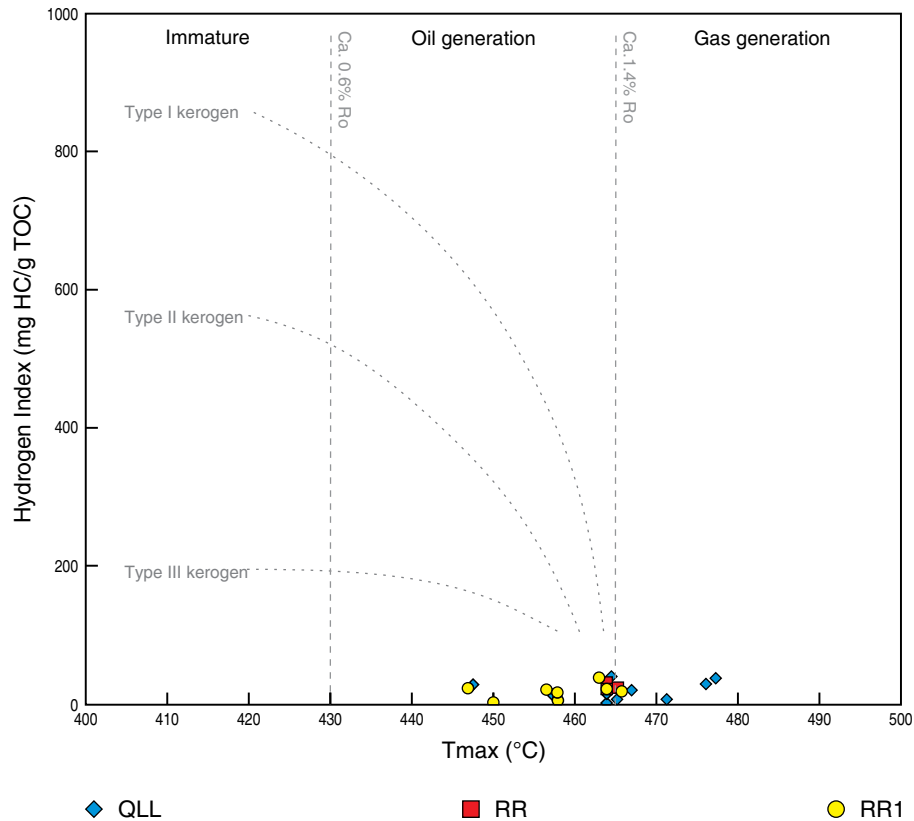


Figure 16. HI vs. Tmax of the Capacho (RR), Guayacán (RR1), and La Luna (QLL, RR1) Formations in the Catatumbo area.

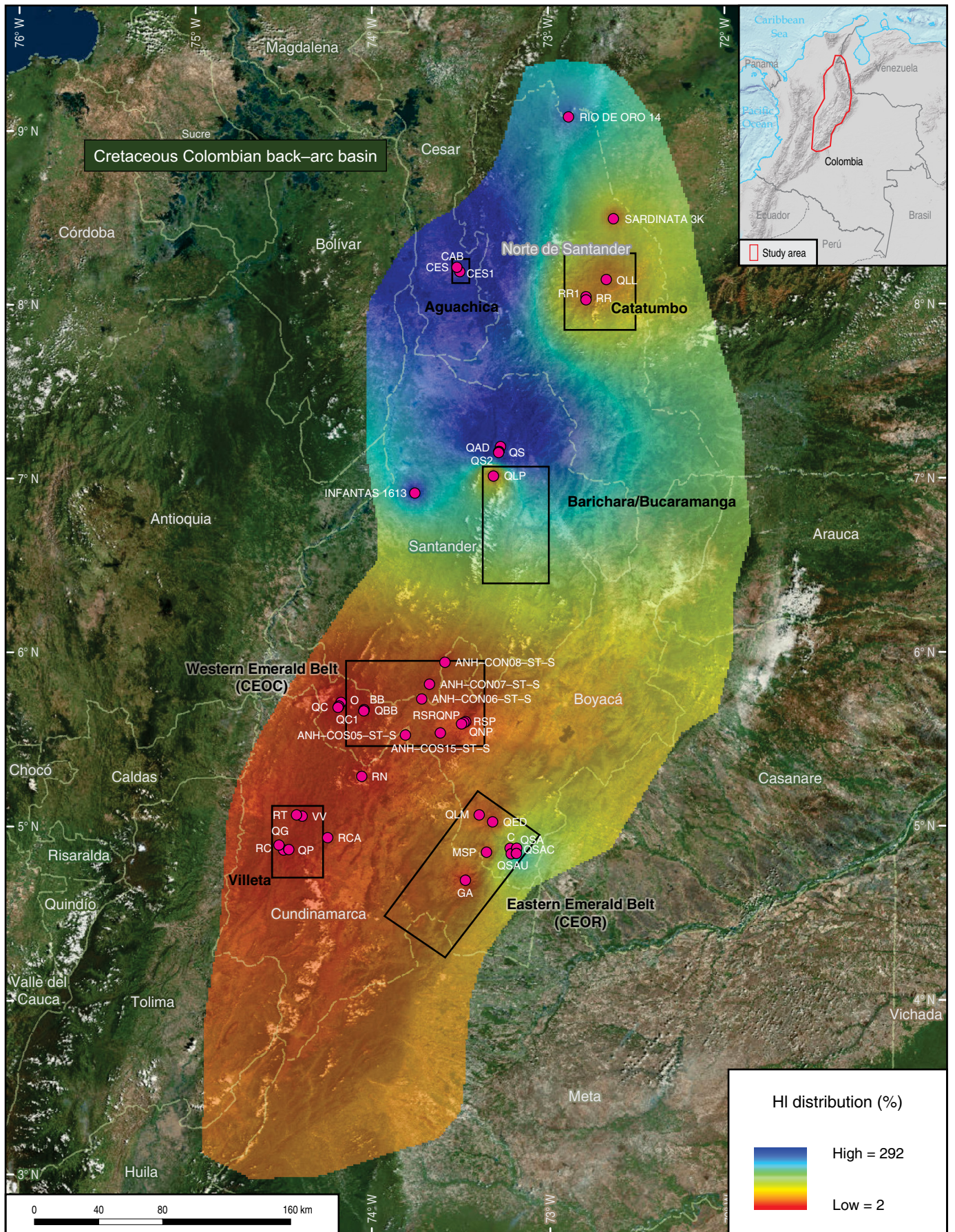




Figure 17. Hydrogen index averages per section. The highest values are present in La Luna Formation from the NW side of the basin, at the MMV and W foothills of the Eastern Cordillera. Total number of samples: 500.

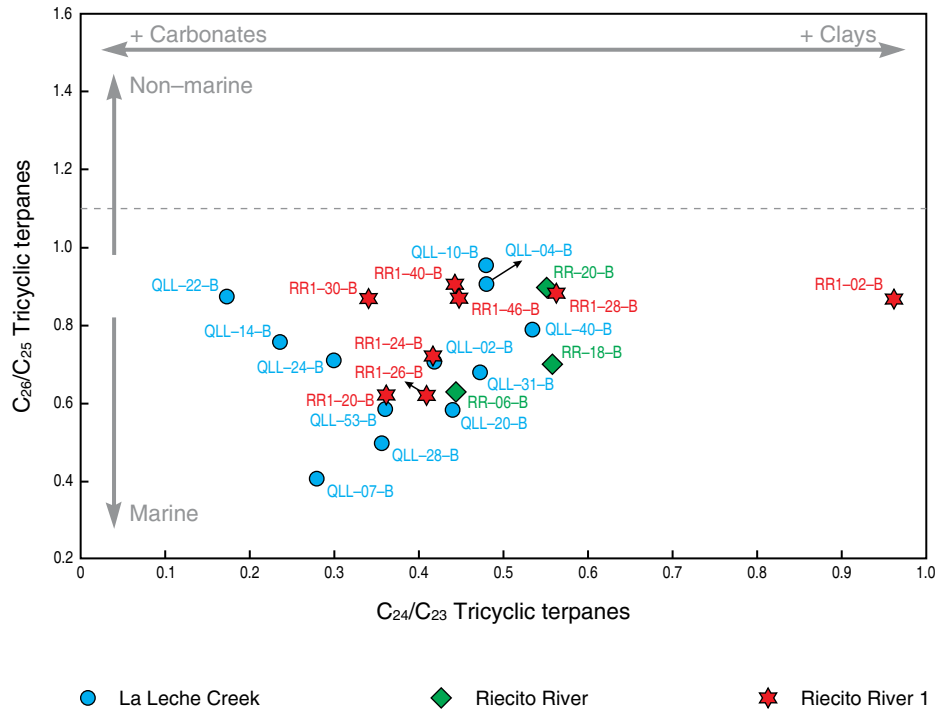


Figure 18. Relationship of tricyclic terpanes indicating the relative presence of marine organic matter related to carbonate rocks versus continental organic matter related to clay mineral content in the Capacho (RR), Guayacán (RR1-02), and La Luna (QLL, RR1) Formations from three localities in the Catatumbo area.

which explain the position of the shale QLP-38 on the right side of the Figure 19, indicating a predominance of continental organic matter. La Luna Formation of the CAB section is composed of partially silicified biomicroites and marlstones composed of foraminifera with 10–80 % calcite, 10–60 % diagenetic quartz, 5–30 % clay minerals, and 5–30 % silt-sized quartz particles. One of the samples toward the right side of the Figure 19, with the highest content of clay minerals (30%), is CAB-50, which is a marlstone and has a mixture of marine and continental organic matter. However, a few samples fall in a field that does not correspond with their lithology.

For instance, the shales of the Simití Formation (QS) contain 35–50 % clay minerals, 40–55 % silt-sized quartz particles, and less than 2% calcite, so they are completely terrigenous and should fall in the field of continental organic matter instead of carbonate marine. The biomicroite limestones of section CES1 have less than 7% clay minerals, so those samples should fall more toward the left, in the carbonate organic matter field, instead of the clay side. In any case, except for the samples mentioned above, the type of organic matter is better expressed by the ratio of tricyclic terpanes than by using the hydrogen index.

Based on mineralogy, fossil content, and organic geochemistry, we conclude that La Luna Formation biomicroite limestones predominantly have type II organic matter of marine origin. Rangel et al. (2017) performed an assessment of the Colombian oils and identified an oil family in the UMV and MMV that suggested an origin in calcareous marine source rocks, which they considered probably related to La Luna Formation limestones.

The mixture of various types of fine-grained rocks (biomicroites, marlstones, and shales) and the type of organic matter (marine versus continental) are very important in the production of unconventional hydrocarbons because they determine the micro scale properties of the rocks, such as fracturing (biomicroites) versus plasticity (marlstones and shales), along with the tendency to produce predominantly oil or gas.

5. Conclusions

The highest average TOC contents of the whole basin correspond to La Luna Formation biomicroites at several localities, including caño El Salto (CES-1) in the Aguachica area in the MMV (11.6% TOC), La Sorda Creek (QS2) section in the

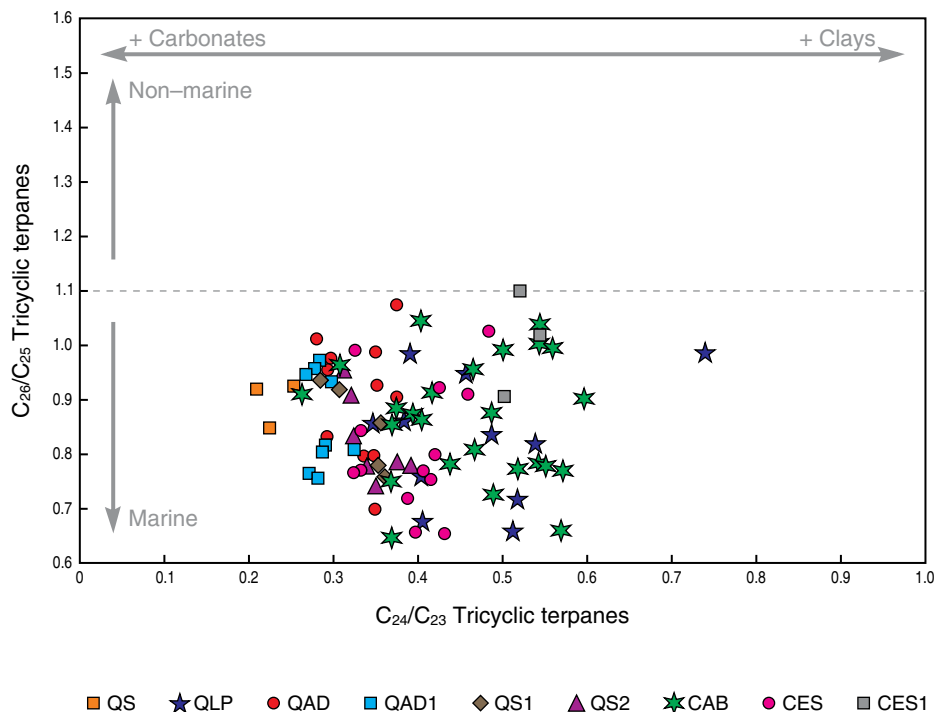


Figure 19. Relationship of tricyclic terpanes indicating the relative presence of marine versus continental organic (carbonate versus clay mineral) content in the Paja (QLP), Simití (QS), and La Luna Formations (QAD, QAD1, CES, CES1, CAB, QS1, QS2) from the MMV.

Barichara area in the W foothills of the Eastern Cordillera (8.6% TOC), and the Rio de Oro oil well (RIO-14) in the Cúcuta/Catatumbo area (8.1% TOC).

Very high TOC values were obtained from individual samples at section CES-1 (21.7% TOC), the Aguadulce Creek (QAD) section in the W foothills of the Eastern Cordillera (18.2% TOC), and caño Aguablanca (CAB) in Aguachica (13.9% TOC). Other units with very high TOC values include La Frontera Member of the Conejo Formation from ANH well COS-5 (24.8% TOC), the Hilo Formation at the Otanche (O) section (12.1% TOC), and the Lomagorda Formation from Cobre Creek (QC) section (7.4% TOC).

The Ro values from La Luna Formation are in the oil and early gas generation windows (0.8–1.3 % Ro). The highest thermal maturity values obtained from pyrolysis are from the Upper Cretaceous Oliní Group (2.4–2.8 % Ro) and Conejo Formation (2.9% Ro). The highest thermal maturity values obtained from vitrinite are from the Lower Cretaceous Murca, Trincheras, and Hilo Formations from the Villeta area (4.0–4.2 % Ro) and the Paja Formation from the Villa de Leyva area (4.3% Ro).

The highest hydrocarbon contents (mainly methane, ethane, and propane) collected in the canister samples cored from field exposures correspond to the Paja, Hilo, Guayacán, La Luna, Lidita Inferior, and Lidita Superior Formations, which contained 1.29 to 5.10 feet³/ton. The samples with the lowest CO₂ contents (3.0–11.5 %) were associated with the highest hydrocarbon contents (15.0–77.8 %). The samples with the

highest gaseous hydrocarbon contents after grinding the samples (residual gas) come from La Luna Formation in La Leche Creek (QLL) and Riecito River (RR1) sections in the Cúcuta/Catatumbo area, La Luna Formation in the caño El Salto (CES1) and caño Aguablanca (CAB) sections in the Aguachica area in the MMV, La Luna Formation in La Sorda Creek (QS2) section in the W foothills of the Eastern Cordillera, the Lidita Inferior and Lidita Superior Formations in the Cobre Creek (QC) and Guate Creek (QG) sections in the W foothills of the Eastern Cordillera, the Paja Formation in La Paja Creek (QLP) section in the western foothills of the Eastern Cordillera, the Hilo Formation in the Contador River (RC) section in the Villeta area, and the Guayacán Formation in the QLL section in the Cúcuta/Catatumbo area.

If the relationship of residual gas of the best samples from La Luna, Paja, and Lidita Inferior Formations (9.1 to 18.1 feet³/ton) is extrapolated to estimate the total gas at depth using an average ratio of total to residual gas of approximately 5 (as found in other basins), they should exhibit total gas values of between 45.5 and 90.5 feet³/ton.

The limestones and cherts of the Guayacán, La Luna, Lidita Inferior, and Lidita Superior Formations, which released the highest average percentages of gaseous hydrocarbons after fracturing and grinding the samples (11.93 to 27.15% of total gas content), have porosity values below 3% and permeability values below 3 microdarcys. The biomicrites and cherts of La Luna Formation have uniform porosities between 1 and 3%,

with permeability values between 0.1 and 11 microdarcys. The biomicrites and cherts of the Lidita Inferior and Lidita Superior also have uniform values of porosity (below 4%) and permeability (below 8 microdarcys). The very low permeability values obtained from the limestones are very good because these mean that the units still retain hydrocarbons in organic matter, nonconnected pores, and fossil cavities, which could be released by fracking.

The pyrolysis and organic geochemistry results reveal that La Luna Formation limestones present the best indicators in terms of hydrocarbon content, type II organic matter, and thermal maturity. The best sections are in the NW sector of the basin, in the areas of Aguachica and Barichara, in the MMV and W foothills of the Eastern Cordillera, followed by the sections from the Catatumbo area in the NE sector of the basin. Older units, with a higher shale and marlstone content, including the Paja, Simití, El Salto, Capacho, and Guayacán, are also in the oil and gas generation windows and have significant amounts of type III and type II kerogen.

Foraminiferal biomicrites, marlstones, and diagenetic cherts have higher contents of TOC than shales, so instead of exploring gas shales, gas biomicrites would constitute a better target. Because the biomicrites have lower or no clay content compared with the claystone and mudstone shales, it is expected that the biomicrites have a more brittle behavior than shales during the process of fracking. In addition, the plastic behavior of the clay shales will more easily close the induced fractures than the biomicrite limestones.

Acknowledgments

We thank the Colombia ANH for permission to publish their data. The field work and analyses were conducted in the frame of project 299–12 to evaluate the nonconventional hydrocarbon potential of fine-grained strata from the Cretaceous Colombian Basin. The project was directed by Javier GUERRERO and supervised by Alejandra MEJÍA–MOLINA. We also appreciate the comments and suggestions of Professor Dr. Yucel AKKUTLU from Texas A&M University and an anonymous reviewer, who helped us to improve the chapter.

References

- Aguilera, R.C., Sotelo, V.A., Burgos, C.A., Arce, C., Gómez, C., Mojica, J., Castillo, H., Jiménez, D. & Osorno, J. 2010. Organic Geochemistry Atlas of Colombia. *Earth Sciences Research Journal*, Special Edition 14, 174 p.
- Casadiago, E. & Rios, C. 2016. Lithofacies analysis and depositional environment of the Galembó Member of La Luna Formation. *Ciencia, Tecnología y Futuro*, 4(1): 37–56.
- Cerón, M.R., Walls, J.D. & Diaz, E. 2013. Comparison of reservoir quality from La Luna, Gacheta, and Eagle Ford Shale Formations using digital rock physics. *Search and Discovery Article 50875*. 15 p.
- Galvis–Portilla, H.A., Higuera–Díaz, I., Cespedes, S., Ballesteros, C., Forero, S., Marfisi, N., Cantisano, M., Pineda, E., Pachon, Z., Slatt, R.M., Ramirez, R., Guzman, G. & Torres, A. 2014. Regional sequence stratigraphy of the Upper Cretaceous La Luna Formation in the Magdalena Valley Basin, Colombia. *Unconventional Resources Technology Conference*, paper 1934959, 10 p. Denver. <https://doi.org/10.15530/URTEC-2014-1934959>
- Guerrero, J. 2002a. A proposal on the classification of systems tracts: Application to the allostratigraphy and sequence stratigraphy of the Cretaceous Colombian Basin. Part 1: Berriasian to Hauterivian. *Geología Colombiana*, (27): 3–25.
- Guerrero, J. 2002b. A proposal on the classification of systems tracts: Application to the allostratigraphy and sequence stratigraphy of the Cretaceous Colombian Basin. Part 2: Barremian to Maastrichtian. *Geología Colombiana*, (27): 27–49.
- Guerrero, J., Sarmiento, G. & Navarrete, R. 2000. The stratigraphy of the W side of the Cretaceous Colombian Basin in the Upper Magdalena Valley. Reevaluation of selected areas and type localities including Aipe, Guaduas, Ortega, and Piedras. *Geología Colombiana*, (25): 45–110.
- Guerrero, J., Mejía–Molina, A. & Osorno, J. 2020. Detrital U–Pb provenance, mineralogy, and geochemistry of the Cretaceous Colombian back–arc basin. In: Gómez, J. & Pinilla–Pachon, A.O. (editors), *The Geology of Colombia, Volume 2 Mesozoic*. Servicio Geológico Colombiano, Publicaciones Geológicas Especiales 36, p. 261–297. Bogotá. <https://doi.org/10.32685/pub.esp.36.2019.08>
- Kennedy, R., Luo, L.X. & Kuuskra, V. 2016. The unconventional basins and plays—North America, the rest of the world, and emerging basins. In: Ahmed, U. & Meehan, D.N. (editors), *Unconventional oil and gas resources: Exploitation and development*. CRC Press, p. 76–111. Boca Raton, USA.
- Liborius, A. & Slatt, R. 2014. Geological characterization of La Luna Formation as an unconventional resource in Lago de Maracaibo Basin, Venezuela. *Unconventional Resources Technology Conference*, paper 2461968. 20 p. Denver, CO, USA. <https://doi.org/10.15530/urtec-2016-2461968>
- Mastalerz, M., Karayigit, A.I., Hampton, L. & Drobniak, A. 2016. Variations in gas content in organic matter–rich low maturity shale; example from the New Albany Shale in the Illinois Basin. *Jacobs Journal of Petroleum and Natural Gas*, 1: 1–16.
- Morales, L.G., Podesta, D., Hatfield, W., Tanner, H.H., Jones, S.H., Barker, M.H.S., O’Donoghue, D.J., Mohler, C.E., Dubois, E.P., Jacobs, C. & Goss, C.R. 1958. General geology and oil occurrences of Middle Magdalena Valley, Colombia: South America. In: Weeks, L.G. (editor), *Habitat of Oil Symposium*. American Association of Petroleum Geologists, p. 641–695. Tulsa, USA.
- Nuñez–Betelu, L. & Baceta, J.I. 1994. Basics and application of rock–eval/TOC pyrolysis: An example from the uppermost

- Paleocene/lowermost Eocene in the Basque Basin, Western Pyrenees. *Natur Zientziak*, (46): 43–62.
- Peters, K.E. & Moldowan, J.M. 1993. *The biomarker guide: Interpreting molecular fossils in petroleum and ancient sediments*. Prentice Hall, 699 p. New Jersey.
- Rangel, A., Osorno, J.F., Ramirez, J.C., De Bedout, J., González, J.L. & Pabón, J.M. 2017. Geochemical assessment of the Colombian oils based on bulk petroleum properties and biomarker parameters. *Marine and Petroleum Geology*, 86: 1291–1309. <https://doi.org/10.1016/j.marpetgeo.2017.07.010>
- Torres, E.J., Slatt, R., Philp, P., O'Brien, N.R.O. & Rodriguez, H.L. 2015. Unconventional resources assessment of La Luna Formation in the Middle Magdalena Valley Basin, Colombia. *Search and Discovery Article 80469*. Denver, CO, USA.
- Veiga, R. & Dzelalija, F. 2014. A regional overview of the La Luna Formation and the Villeta Group as shale gas/shale oil in the Catatumbo, Magdalena Valley and Eastern Cordillera Regions, Colombia. *Search and Discovery Article 10565*. Cartagena.
- Walls, J.D., Cerón, M.R. & Anderson, J. 2014. Characterizing unconventional resource potential in Colombia; a digital rock physics project. *Unconventional Resources Technology Conference*, paper 1913256, 9 p. Denver. <https://doi.org/10.15530/urtec-2014-1913256>
- Zumberge, J. 1984. Source rocks of the La Luna Formation (Upper Cretaceous) in the Middle Magdalena Valley, Colombia. In: Palacas, J. (editor), *Petroleum Geochemistry and Source Rock Potential of Carbonate Rocks*. American Association of Petroleum Geologists, Special volumes, 18, p. 127–133.

Explanation of Acronyms, Abbreviations, and Symbols:

ANH	Agencia Nacional de Hidrocarburos	RST	Regressive systems tract
HC	Hydrocarbon	SEM	Scanning Electron Microscope
HI	Hydrogen index	Tmax	Temperature of maximum hydrocarbon generation
HST	Highstand systems tract	TOC	Total organic carbon
ICP–MS	Inductively coupled plasma mass spectrometry	TST	Transgressive systems tract
MMV	Middle Magdalena Valley	UMV	Upper Magdalena Valley
MORB	Mid–ocean ridge basalt	XRD	X–ray diffraction
PI	Production index		
Ro	Thermal maturity		

Authors' Biographical Notes



Javier GUERRERO is a geologist from the Universidad Nacional de Colombia. He obtained a Master of Science degree and a PhD from Duke University (USA) in the areas of stratigraphy, sedimentology, and paleomagnetism. He participated with a multidisciplinary group of geologists and paleontologists from several American universities in a project on biostratigraphy, sedimentology, and mag-

netostratigraphy of the Honda Group in the Tatacoa Desert. He worked at the stratigraphy section of the Servicio Geológico Colombiano on various projects on the Cenozoic from the Magdalena River Valley. Recently, he has been a professor in the Departamento de Geociencias at the Universidad Nacional de Colombia, lecturing in courses on sedimentology, sequence stratigraphy, and regional geology. Javier has conducted research and consulting projects for several petroleum companies and for the Agencia Nacional de Hidrocarburos (ANH) on rocks of the Cretaceous Colombian back–arc basin and the Cenozoic foreland basin.



Alejandra MEJÍA–MOLINA is a geologist from the Universidad de Caldas (Colombia) who has been working during the last decade in paleontology, paleoecology, paleoceanography, and paleoclimatology as a member of the Grupo de Geociencias Oceánicas (GGO) at the Universidad de Salamanca (España). Her Master's thesis was on Quaternary marine/continental variability in North

Africa and her Doctoral thesis was on calcareous nannofossils, both at the Universidad de Salamanca. Alejandra worked for the Agencia Nacional de Hidrocarburos (ANH) on several projects to obtain new geological data and evaluate the Colombian exploratory potential of both conventional (Pacific and Caribbean offshore basins) and unconventional hydrocarbons (Cretaceous from the Eastern Cordillera). She currently works for the Escuela de Ciencias Geológicas e Ingeniería at the Universidad Yachay Tech, Ecuador.



José OSORNO is a geologist from the Universidad de Caldas with a specialization in project management from the Universidad Piloto de Colombia. He recently completed a Master of Science in energy management at Universidad Sergio Arboleda and an Executive MBA at the Universitat Politècnica de València, España. José Fernando worked for 18 years at the Servicio Geológico Colombiano in the División de Geología Regional y Estratigrafía. Recently, he has been working at the Agencia Nacional de Hidrocarburos (ANH) in project design and evaluation, including the definition of oil systems in Colombia and geochemical evaluation of the Sinú–San Jacinto area. He is currently responsible for “yet-to-find” projects focused on calculating the potential of hydrocarbons yet to be discovered in the sedimentary basins of Colombia. José is also responsible for projects on the potential of unconventional hydrocarbons in the country.

